

Complex-Temperature Properties of the Ising Model on 2D Heteropolygonal Lattices

Victor Matveev* and Robert Shrock**

Institute for Theoretical Physics
State University of New York
Stony Brook, N. Y. 11794-3840

Abstract

Using exact results, we determine the complex-temperature phase diagrams of the 2D Ising model on three regular heteropolygonal lattices, $(3 \cdot 6 \cdot 3 \cdot 6)$ (kagomé), $(3 \cdot 12^2)$, and $(4 \cdot 8^2)$ (bathroom tile), where the notation denotes the regular n -sided polygons adjacent to each vertex. We also work out the exact complex-temperature singularities of the spontaneous magnetisation. A comparison with the properties on the square, triangular, and hexagonal lattices is given. In particular, we find the first case where, even for isotropic spin-spin exchange couplings, the nontrivial non-analyticities of the free energy of the Ising model lie in a two-dimensional, rather than one-dimensional, algebraic variety in the $z = e^{-2K}$ plane.

*email: vmatveev@max.physics.sunysb.edu

**email: shrock@max.physics.sunysb.edu

1 Introduction

The Ising model has long served as a prototype of a statistical mechanical system which undergoes a phase transition with associated spontaneous symmetry breaking and long range order. The Ising model on a dimension $d = 2$ lattice has the great appeal that (for the spin $1/2$ case with nearest-neighbor interactions) it is exactly solvable; for the square lattice, in the absence of an external magnetic field H , the free energy was first calculated by Onsager [1], and a closed-form expression for the spontaneous magnetisation was first derived by Yang [2]. Later, the zero-field model was also solved for the triangular and hexagonal (= honeycomb) lattices; for a comparative review of the solutions on these three lattices, see Ref. [3]. However, in addition to the square, triangular, and hexagonal lattices, which involve tilings of the plane by one type of regular polygon, there are also other 2D lattices which have the property that all vertices are equivalent and all links (bonds) are of equal length, but are comprised of tilings by more than one type of regular polygons. We shall denote the regular 2D lattices which are comprised of tilings by one type of polygon as “homopolygonal” and those involving tilings by more than one type of polygon as “heteropolygonal”. Indeed, as will be discussed further below, the (zero-field) free energy and spontaneous magnetisation for the Ising model have been calculated for three heteropolygonal 2D lattices. The results yield valuable insights into how the properties of the solution depend on the tiling of the plane and, in particular, how they change when this tiling involves more than one kind of polygon.

In the present paper, we shall determine the complex-temperature phase diagrams and singularities of the spontaneous magnetisation for the three particular heteropolygonal lattices for which the Ising model has been solved. There are several reasons for studying the properties of statistical mechanical systems such as spin models with the temperature variable generalised to take on complex values. First, one can understand more deeply the behaviour of various thermodynamic quantities by seeing how they behave as analytic functions of complex temperature. Second, one can see how the physical phases of a given model generalise to regions in appropriate complex-temperature variables. Third, a knowledge of the complex-temperature singularities of quantities which have not been calculated exactly helps in the search for exact, closed-form expressions for these quantities. This applies, in particular, to the susceptibility of the 2D Ising model. Complex-temperature properties of the Ising model (zeros of the partition function and singularities of thermodynamic and response functions) have been explored in a number of papers for homopolygonal 2D lattices and for various 3D lattices [4, 5, 6, 7, 8, 9, 10, 11, 12, 13, 14]. (Refs. [8] and part of Refs. [5, 6] deal with the $d = 3$ Ising model.) However, to our knowledge, analogous investigations

of complex-temperature properties have not been reported for heteropolygonal 2D lattices.

To begin, we need to describe the heteropolygonal lattices. We shall use the standard mathematical notation for general lattices [15]. An important virtue of this notation is that the mathematical symbol explicitly contains sufficient information for one to reconstruct the lattice. A regular tiling of the plane is defined as one involving one or more regular polygons, i.e. polygons each of whose sides are of equal length. An Archimedean lattice is defined as a regular tiling of the plane in which all vertices are equivalent. Thus each vertex has the same coordination number, which we shall denote as q . From the definition, it follows immediately that all of the links on an Archimedean lattice are of equal length. For this reason, it is natural to consider the case of equal spin-spin couplings, and we shall do this here. However, it should be noted that the links on an Archimedean lattice are not, in general, all equivalent. For the three homopolygonal Archimedean lattices, it is obvious that all links are equivalent, but for the heteropolygonal lattices, this equivalence only holds if (a) the lattice consists of only two types of polygons and (b) each edge of the first type of polygon is also an edge of the second type of polygon. Among the eight heteropolygonal Archimedean lattices, this condition is met only for the $(3 \cdot 6 \cdot 3 \cdot 6)$ (kagomé) lattice (see below). The mathematical definition of, and notation for, an Archimedean lattice Λ are specified by

$$\Lambda = \left(\prod_{j=1}^q p_j \right) \quad (1.1)$$

where p denotes a regular p -gon. The meaning of eq. (1.1) is that as one makes a small circuit around any vertex, one traverses first the polygon p_1 , next p_2 , and so forth, finally traversing p_q . Because the starting point is irrelevant, the symbol is invariant under cyclic permutations:

$$(p_1 \cdot p_2 \cdots p_q) = (p_2 \cdot p_3 \cdots p_q \cdot p_1) \quad (1.2)$$

and so forth for other cyclic permutations. If a p -sided polygon occurs ℓ times sequentially in this product, one signifies this by p^ℓ . There are 11 such ($d = 2$) Archimedean lattices [15]. Of the 11 Archimedean lattices, three are homopolygonal. These are the well-known square, triangular, and hexagonal lattices, which are denoted, respectively, (4^4) , (3^6) , and (6^3) . Note that the dual of a homopolygonal lattices (p^ℓ) is (ℓ^p) , so that it is self-dual if and only if $p = \ell$, which occurs only for $p = 4$. The other eight Archimedean lattices are heteropolygonal. The full set of these lattices is listed in Table 1. (One lattice, $(3^4 \cdot 6)$, occurs in two enantiomorphic (chiral) forms, which are considered together in this counting.)

The three heteropolygonal Archimedean lattices for which we shall determine the complex-temperature phase diagrams and singularities of the magnetisation are those for which the Ising model has been solved exactly, namely the (i) $(3 \cdot 6 \cdot 3 \cdot 6)$, (ii) $(3 \cdot 12^2)$, and (iii) $(4 \cdot 8^2)$

| lattice | name | q | bip. | sym. |
|---------------------------------|---------------|-----|------|---------------------------------------|
| (3^6) | triangular | 6 | N | $z \rightarrow -z$ |
| (4^4) | square | 4 | Y | $z \rightarrow -z, z \rightarrow 1/z$ |
| (6^3) | hexagonal | 3 | Y | $z \rightarrow 1/z$ |
| $(3 \cdot 6 \cdot 3 \cdot 6)$ | kagomé | 4 | N | $z \rightarrow -z$ |
| $(3 \cdot 12^2)$ | — | 3 | N | n |
| $(4 \cdot 8^2)$ | bathroom tile | 3 | Y | $z \rightarrow 1/z$ |
| $(3^4 \cdot 6)$ | — | 5 | N | n |
| $(3^3 \cdot 4^2)$ | — | 5 | N | n |
| $(3^2 \cdot 4 \cdot 3 \cdot 4)$ | — | 5 | N | n |
| $(3 \cdot 4 \cdot 6 \cdot 4)$ | — | 4 | N | $z \rightarrow -z$ |
| $(4 \cdot 6 \cdot 12)$ | — | 3 | Y | $z \rightarrow 1/z$ |

Table 1: Table of the 11 Archimedean lattices. The first three are the well-known homopolygonal ones, and the remaining eight are heteropolygonal. The entries in the column denoted bip. indicate whether (Y,N) the lattice is bipartite. The entries in the column denoted “sym.” indicate whether the complex-temperature phase diagram and zeros of the partition function for the (spin 1/2, zero-field) Ising model have the symmetries $z \rightarrow -z$ and/or $z \rightarrow 1/z$, or neither, denoted by “n”.

lattices. For the reader's convenience, these lattices are shown in Figs. 1-3, respectively. The $(3 \cdot 6 \cdot 3 \cdot 6)$ lattice is often called the kagomé lattice, after a Japanese word for a similar type of basket weave. The $(4 \cdot 8^2)$ lattice is often called the bathroom tile lattice. In the literature, the $(3 \cdot 12^2)$ and $(4 \cdot 8^2)$ lattices are frequently denoted by the shorthand symbols $3 - 12$ and $4 - 8$. As was observed by Utiyama [16], one way to construct these lattices is to start from a checkerboard lattice, replace each "black" square by a square with n_v additional vertical bonds, and then take certain of the spin-spin couplings either to 0 or ∞ . One chooses $n_v = 1$ to construct the $(3 \cdot 6 \cdot 3 \cdot 6)$ and $(4 \cdot 8^2)$ lattices, and $n_v = 3$ to construct the $(3 \cdot 12^2)$ lattice. Using this observation, Utiyama discussed ingredients for an exact solution for the (zero-field) free energy for these lattices [16]. These lattices can also be obtained by (possibly iterated) decoration and/or star-triangle operations from the three homopolygonal lattices [17].

We recall that abstractly, the duality mapping for a d -dimensional lattice maps k -cells to $d-k$ cells. In our present case, with $d = 2$, this mapping interchanges 0-cells (vertices) and 2-cells (polygonal faces) while taking 1-cells (links) to other links. The duals of Archimedean lattices are Archimedean if and only if they are homopolygonal; for the heteropolygonal Archimedean lattices, the dual lattices are of a different type, called Laves lattices in the mathematical literature [15, 18]. A Laves lattice is defined as a regular tiling of the plane involving a single (in general, non-regular) polygon. Thus, the links of a Laves lattice are not, in general, of equal length, and the vertices (sites) are not, in general, equivalent. There is a one-to-one correspondence, namely that of duality, between the 11 Archimedean lattices and the 11 Laves lattices. Clearly, the number of different types of 0-cells (vertices) on the Laves lattice Λ^* which is the dual of the Archimedean lattice Λ is equal to the number of different 2-cells (polygons) on Λ . Similarly, the fact that the Laves lattice consists of only one type of (generally non-regular) 2-cell (polygon) follows, by duality, from the fact that its dual Archimedean lattice consists of only one type of 0-cell (vertex). The standard mathematical notation for a Laves lattice Λ is

$$\Lambda = [(\prod_{j=1}^p q_j)] \quad (1.3)$$

the meaning of which is as follows: on a given polygon, as one makes a circuit around its periphery, one passes first a vertex with coordination number q_1 , next a vertex with coordination number q_2 , and so forth, finally coming to a vertex with coordination number q_p , where p denotes the number of (generally non-equal) sides of the polygon, which is, of course, equal to the number of vertices of this polygon. The Laves lattice $[(\prod_{j=1}^p q_j)]$ is the dual of the Archimedean lattice $(\prod_{j=1}^q p_j)$ for $p = q$ and $p_j = q_j$, $j = 1 \dots p$. As an example, the Laves lattice $[4 \cdot 8^2]$ (commonly called the union jack lattice) is shown in Fig.

4 and is evidently the dual of the Archimedean lattice $(4 \cdot 8^2)$ (bathroom tile). From the duality relation with the Archimedean lattices, or directly from the definition, it follows that there are three Laves lattices for which the vertices are, in fact, all equivalent; these are $[3^6]$, $[4^4]$, and $[6^3]$. We shall denote these as homoverticial, and the remaining eight Laves lattices with inequivalent vertices as heteroverticial, by analogy with the homopolygonal and heteropolygonal Archimedean lattices.

The solution for the (zero-field) free energy on each of the Archimedean lattices immediately gives the solution on the corresponding dual Laves lattice. Thus, our determination of the complex-temperature phase diagrams for the three heteropolygonal Archimedean lattices considered here also yields a corresponding determination of the complex-temperature phase diagrams for their dual Laves lattices.

2 Model and Notation

Our notation is standard, so we review it here only briefly. We consider the spin 1/2 Ising model on the 2D lattices Λ as discussed above at a temperature T and external magnetic field H (where $H = 0$ unless otherwise specified) defined by the partition function

$$Z = \sum_{\{\sigma_n\}} e^{-\beta\mathcal{H}} \quad (2.1)$$

with the Hamiltonian

$$\mathcal{H} = -J \sum_{\langle nn' \rangle} \sigma_n \sigma_{n'} - H \sum_n \sigma_n \quad (2.2)$$

where $\sigma_n = \pm 1$ are the Z_2 spin variables on each site n of the lattice Λ , $\beta = (k_B T)^{-1}$, J is the exchange constant, $\langle nn' \rangle$ denote nearest-neighbour sites, and the units are defined such that the magnetic moment which would multiply the $H \sum_n \sigma_n$ is unity. (Hereafter, we shall use the term “Ising model” to denote the spin 1/2 Ising model unless otherwise indicated.) We use the usual notation $K = \beta J$, $h = \beta H$, $v = \tanh K$, $z = e^{-2K}$, $u = z^2 = e^{-4K}$, and $\mu = e^{-2h}$. Note that v and z are related by the bilinear conformal transformation

$$z = \frac{1-v}{1+v} \quad (2.3)$$

We record the symmetries

$$K \rightarrow -K \Rightarrow \{v \rightarrow -v, \quad z \rightarrow 1/z, \quad u \rightarrow 1/u\} \quad (2.4)$$

It will also be useful to introduce the common abbreviations

$$C \equiv \cosh(2K) \quad (2.5)$$

$$S \equiv \sinh(2K) \tag{2.6}$$

The reduced free energy per site is $f = -\beta F = \lim_{N_s \rightarrow \infty} N_s^{-1} \ln Z$ in the thermodynamic limit, where N_s denotes the number of sites on the lattice.

3 Some Basic Properties

We begin by discussing the phase boundaries of the model as a function of complex temperature, i.e. the locus of points across which the free energy is non-analytic. The physical phases of the model include the phase where the Z_2 symmetry is realised explicitly, viz., the paramagnetic (PM) phase, and also, for dimension greater than the lower critical dimensionality (i.e., $d \geq 2$, for integer d), a phase where the Z_2 symmetry is spontaneously broken with long-range ferromagnetic (FM) order, i.e. a nonzero spontaneous (uniform) magnetisation, M . For the lattices considered here which are bipartite and hence involve no frustration for antiferromagnetic (AFM) ordering, there is also a phase with AFM long range order, i.e. a nonzero staggered magnetisation, M_{st} . As one can see from Table 1, of the three heteropolygonal lattices considered here, only the $(4 \cdot 8^2)$ lattice is bipartite. One defines the complex-temperature extensions of the physical phases by analytic continuation in K or an equivalent variable such as v , z , or u . There are, in general, also complex-temperature phases which have no overlap with any physical phase. As in our earlier work, we label these as O phases (where O denotes “other”), including subscripts to distinguish them where there are several. In cases where one O phase is precisely the complex conjugate of another, we label the one with $Im(z) \geq 0$ by O (with subscript where necessary) and its complex conjugate by O^* . (From eq. (2.3), it follows that in the v plane, the corresponding O and O^* phases have $Im(v) \leq 0$ and $Im(v) \geq 0$, respectively.)

As noted in Ref. [9], there is an infinite periodicity in complex K under the shift $K \rightarrow K + ni\pi$, where n is an integer, and, for lattices with even coordination number q , also the shift $K \rightarrow (2n + 1)i\pi/2$, as a consequence of the fact that the spin-spin interaction $\sigma_n \sigma_{n'}$ in \mathcal{H} is an integer. In particular, there is an infinite repetition of phases as functions of complex K . These repeated phases are reduced to a single set by using the variables v , z or u , owing to the symmetry relation $K \rightarrow K + ni\pi \Rightarrow \{v \rightarrow v, z \rightarrow z, u \rightarrow u\}$. It is thus convenient to use these variables here.

As we have discussed in our earlier works [11, 12, 13], the equations for the locus of points where the free energy is non-analytic also serve to define the boundaries of the complex-temperature phases of the model. Some of the loci of points where the free energy is non-analytic do not actually separate any phases, but rather are arcs or line segments protruding

into various phases. In passing we note that the free energy is, of course, also trivially non-analytic at $K = \pm\infty$, i.e. $v = \pm 1$ or $z = 0, \infty$. This is obvious from eqs. (2.1) and (2.2). Because these points are isolated, they do not separate any complex-temperature phases and hence will not be important here.

Before proceeding, we list some theorems which formalise results in our earlier work. Although these are elementary, it will be useful to record them here for our later discussion of the complex-temperature phase diagrams. Some of the theorems will be given in greater generality than is needed here.

Theorem 1

Consider the (spin 1/2, zero-field) Ising model on an arbitrary lattice. The loci of points in the complex z and v planes where the free energy of the Ising model is non-analytic are symmetric under complex conjugation, i.e. under reflection about the $Im(z) = 0$ and $Im(v) = 0$ axes, respectively. Hence the same is true of the complex-temperature phase boundaries in these variables. The same is also true of the zeros of the partition function on finite lattices.

Proof

One can prove the first two parts of this theorem either by starting with finite lattices or by considering only the properties of the thermodynamic limit. If one uses finite lattices, this automatically also proves the last part of the theorem, concerning zeros of the partition function. The basic property that one uses is that the partition function on a finite lattice is a generalised polynomial. (Here, a “generalised polynomial” in the variable ζ is defined as function consisting of a finite sum of integral powers of ζ , where negative as well as positive powers are allowed. Specifically, the partition function has the form

$$Z = \sum_{p=-N_\ell/2}^{N_\ell/2} c_p z^p \tag{3.1}$$

where N_ℓ denotes the number of links on the lattice and the c_p are real. (In fact, c_p are not just real, but integral, and also satisfy the symmetry $c_p = c_{N_\ell-p}$, but these properties will not be needed here.) The zeros of Z are the zeros of the polynomial

$$P(z) = z^{N_\ell/2} Z = \sum_{p=0}^{N_\ell} c_p z^p \tag{3.2}$$

Since the polynomial $P(z)$ has real coefficients, it satisfies

$$P(z)^* = P(z^*) \quad (3.3)$$

Hence, if z_j is a zero of $P(z)$, then so is z_j^* . This proves the third part of the theorem, on the zeros of the partition function for finite lattices. Taking the thermodynamic limit, one obtains the result that the non-analyticities of the free energy and hence the complex-temperature phase boundaries, are invariant under $z \rightarrow z^*$. From the mapping (2.3) relating z and v , the same result follows for the non-analyticities and phase boundaries in the v plane.

□

In passing, we note that if one uses periodic boundary conditions, then the number of links is simply given by $N_\ell = (q/2)N_s$. Moreover, for the part of the theorem which deals with the free energy (in the thermodynamic limit), an alternate way of seeing the result is to observe that f has the form

$$f = \ln 2 + \int_{-\pi}^{\pi} \int_{-\pi}^{\pi} \frac{d\theta_1 d\theta_2}{(2\pi)^2} \ln[A + B(\theta_1, \theta_2)] \quad (3.4)$$

where A and B are rational functions of z , or equivalently, v , with real coefficients. Aside from isolated points at $K = \pm\infty$ (i.e., $v = \pm 1$, $z = 0, \infty$) and, for odd q , the point $z = -1$, the above locus of points is the set where $A + B(\theta_1, \theta_2) = 0$. But since this amounts to a polynomial equation in z or v with real coefficients, it follows that the roots of the equation are either real or come in complex conjugate pairs.

This theorem can be generalised in two ways. Although we shall not need either of these generalisations here, we state them for completeness. First, the theorem actually applies not just for the case of zero external field, but also for the case of nonzero (real) magnetic field. One can also show that it is true for pure imaginary h . Secondly, one can straightforwardly generalise Theorem 1 to the case of the spin s Ising model. For this purpose, we define the normalisation of the spin values to be $\sigma_n \in \{-2s, -2s+2, \dots, 2s-2, 2s\}$ in eqs. (2.1) and (2.2). Then the generalisation of Theorem 1 reads as given there, without the restriction to spin 1/2. For integral s , a commonly used alternate normalisation is $\sigma_n \in \{-s, -s+1, \dots, s-1, s\}$; with this normalisation, the generalisation of Theorem 1 would use the modified definition $z = e^{-K}$.)

Theorem 2

For the (spin 1/2, zero-field) Ising model, if and only if the lattice has even coordination number $q = 2r$, the complex-temperature phase diagram is invariant under the transformation $z \rightarrow -z$. The same is true of the zeros of the partition function for finite lattices.

Proof

This follows by explicit calculation of the partition function for finite lattices. For odd q , Z is a generalised polynomial in z , while for even q , it is a generalised polynomial in $u = z^2$. Using the definition of the free energy $f = \lim_{N_s \rightarrow \infty} N_s^{-1} \ln Z$, it follows that the locus of points where the free energy is non-analytic has the same symmetry. \square

Thus, for lattices with even q , a more compact way to display the complex-temperature phase diagram is in the complex u plane.

Theorem 3

For the (spin 1/2, zero-field) Ising model, if and only if the lattice is bipartite, the complex-temperature phase diagram is invariant under the transformation $z \rightarrow 1/z$ ($u \rightarrow 1/u$ if also q is even). The same is true of the zeros of the partition function for finite lattices.

Proof

The statement that the lattice is bipartite means that it can be decomposed into two sublattices, which we may denote as even (e) and odd (o), such that each site on the even sublattice has as its nearest neighbors only sites on the odd sublattice, and vice versa. Since the spin-spin interaction in the Hamiltonian only involves nearest-neighbor pairs, it follows that under the mapping

$$\begin{aligned} \sigma_e &\rightarrow \sigma_e \\ \sigma_o &\rightarrow -\sigma_o \\ J &\rightarrow -J \end{aligned} \tag{3.5}$$

the partition function Z and hence also the free energy f are invariant, where σ_e and σ_o denote spins on the even and odd sublattices. Hence

$$Z(K) = Z(-K), \quad f(K) = f(-K) \tag{3.6}$$

The theorem follows, since $K \rightarrow -K$ is equivalent to $z \rightarrow 1/z$. \square

Theorem 4

In the z plane, the zeros (and any divergences) of the spontaneous magnetisation M occur at either real values or at complex conjugate pairs of values.

Proof

Theorem 4 is a corollary of the generalisation of Theorem 1 to the case of nonzero (real) external field h . Since $M = \lim_{H \rightarrow 0} \partial M / \partial h$, this generalisation of Theorem 1 implies that

$$M(z)^* = M(z^*) \quad (3.7)$$

Hence, in particular, the set of zeros of M as a function of z is invariant under $z \rightarrow z^*$. Similarly, the set of values of z where M diverges (if this set is non-null) is invariant under $z \rightarrow z^*$. \square

The following result is a corollary of this theorem:

Theorem 5

On a bipartite lattice, in the $w = 1/z$ plane, the zeros (and any divergences) of the spontaneous staggered magnetisation M_{st} occur at either real values or at complex conjugate pairs of values.

Proof

This theorem follows from the fact that the symmetry (3.5) maps the model with the ferromagnetic sign of the spin-spin coupling, $J > 0$, to the model with the antiferromagnetic sign, $J < 0$. This allows one to obtain the staggered magnetisation M_{st} immediately from the uniform magnetisation; in the physical AFM phase and, by analytic continuation, throughout the full complex-temperature extension of the AFM phase, M_{st} is given as

$$M_{st}(w) = M(z \rightarrow w) \quad (3.8)$$

where $w = 1/z = e^{2K} = e^{-2|K|}$. (M_{st} vanishes identically elsewhere.) \square

Theorem 6

For lattices with odd coordination number q , the zero-field partition function Z of the (spin 1/2) Ising model vanishes at $z = -1$, and the free energy contains a negatively divergent singularity at this point.

Proof

From the definition of the partition function and of K , we have

$$Z = \sum_{\{\sigma_n\}} \exp(K \sum_{\langle nn' \rangle} \sigma_n \sigma_{n'}) \quad (3.9)$$

Now, in general, for each link $\langle nn' \rangle$, since $\sigma_n \sigma_{n'} = \pm 1$, it follows that

$$e^{K\sigma_n \sigma_{n'}} = \cosh K + \sigma_n \sigma_{n'} \sinh K \quad (3.10)$$

The K values corresponding to $z = \lim_{\epsilon \rightarrow 0} (-1 \pm \epsilon)$ (where ϵ denotes a small real number) are $K = -(1/2) \lim_{\epsilon \rightarrow 0} \ln(-1 \pm \epsilon) = -(1/2)(\pm i\pi + 2ni\pi)$, where we follow the usual convention of taking the branch cut for $\log z$ to lie along the negative real z axis, and n indexes the Riemann sheet of the logarithm. To minimize unimportant minus signs, we consider $z = \lim_{\epsilon \rightarrow 0} (-1 - \epsilon)$ and take the principal Riemann sheet of the log, $n = 0$; then $K = i\pi/2$. Substituting this into eq. (3.10), we have

$$e^{(i\pi/2)\sigma_n \sigma_{n'}} = i\sigma_n \sigma_{n'} \quad (3.11)$$

so that

$$Z = \sum_{\{\sigma_n\}} \left(\prod_{\langle nn' \rangle} i\sigma_n \sigma_{n'} \right) \quad (3.12)$$

Since the lattice has coordination number q , in this product over all links, the σ_n for each site n appears q times, and hence eq. (3.12) can be rewritten as a product over all sites:

$$Z = i^{N_\ell} \sum_{\{\sigma_n\}} \left(\prod_n \sigma_n^q \right) \quad (3.13)$$

Evaluating the summation over each spin, we have

$$Z = i^{N_\ell} \left[(+1)^q + (-1)^q \right]^{N_s} \quad (3.14)$$

Evidently, for odd q , the summation over $\sigma_n = \pm 1$ on each site yields 0, and hence $Z = 0$, so that the free energy is negatively divergent at this point. \square

Among the lattices considered here, the hexagonal, $(3 \cdot 12^2)$, and $(4 \cdot 8^2)$ ones have odd q (in each case, $q = 3$), so that Theorem 6 implies that the respective free energy f for each has a divergent singularity at $z = -1$.

From eq. (3.14) in the proof of Theorem 6, it is immediately evident that for the (spin 1/2) Ising model on a lattice of even $q = 2r$, the value of the partition function on a finite lattice with periodic boundary conditions (and hence the relation $N_\ell = (q/2)N_s$) is

$$Z(z = -1; q = 2r) = i^{rN_s} 2^{N_s} \quad (3.15)$$

while the (reduced) free energy satisfies

$$f(z = -1; q = 2r) = r \ln i + \ln 2 \quad (3.16)$$

(independent of boundary conditions, since these do not affect the thermodynamic limit). In eq. (3.16), $\ln i = i\pi/2 + 2\pi in$, where n labels the Riemann sheet of the log.

The points across which the free energy is non-analytic are related to the zeros of the partition function. A fundamental question concerns whether these points (apart from the trivial ones at $K = \pm\infty$ and, for odd q , at $z = -1$ as proved in Theorem 6) lie on curves (including line segments) in the z (or equivalently, v) plane, or whether they lie in areas. For homopolygonal 2D lattices with isotropic spin-spin exchange couplings, these points do lie on curves. (There is also numerical evidence for this in the case of 3D lattices [8].) It is also well known that for 2D homopolygonal lattices with anisotropic couplings, these points lie, in general, in areas rather than on curves [19]. It is worthwhile to investigate this question for heteropolygonal lattices, and we shall do so, as part of our general determination of the complex-temperature phase diagrams. Indeed, one of our interesting results will be the finding that even for isotropic spin-spin couplings, the zeros do not always lie on curves in the case of heteropolygonal lattices. We shall give a simple explanation of this finding below.

We now proceed with our analyses.

4 (3 · 6 · 3 · 6) Lattice

The (zero-field) free energy of the Ising model on the (3 · 6 · 3 · 6) (kagomé) lattice with equal spin-spin couplings was first calculated explicitly by Kano and Naya [20]. The result is

$$f_{kag.} = \ln 2 + \frac{1}{6} \int_{-\pi}^{\pi} \int_{-\pi}^{\pi} \frac{d\theta_1 d\theta_2}{(2\pi)^2} \ln \left\{ \frac{1}{4} [(C^3 + S^3)^2 + 3C^2 - 2CS^2(C + S)P(\theta_1, \theta_2)] \right\} \quad (4.1)$$

where

$$P(\theta_1, \theta_2) = \cos(\theta_1) + \cos(\theta_2) + \cos(\theta_1 + \theta_2) \quad (4.2)$$

As was the case with the homopolygonal lattices, the connected locus of points across which the free energy is non-analytic is the set of points for which the logarithm in the integral of eq. (4.1) vanishes. These are also the zeros of the partition function. In terms of the variable u , this vanishing condition is the equation

$$(21u^4 + 24u^3 + 18u^2 + 1) - 4u(1 + u)(1 - u)^2 x = 0 \quad (4.3)$$

where x represents $P(\theta_1, \theta_2)$ and takes values in the range

$$-\frac{3}{2} \leq x \leq 3 \quad (4.4)$$

For $x = 3$, there is a double real root at $u_{c,kag.}$, where

$$u_{c,kag.} = -1 + \frac{2}{\sqrt{3}} \simeq 0.15470054... \quad (4.5)$$

and another double real root at $-1/(3u_{c,kag.}) = -1 - 2/\sqrt{3}$. As indicated in the notation, $u_{c,kag.}$ is the physical critical point separating the FM and PM phases. As x decreases from 3 in the range $-1 < x < 3$, each of these splits into two pairs, which trace out the curves in Fig. 5(a). For $x = -1$, these rejoin in conjugate double roots at the multiple or intersection points u_k and u_k^* , where

$$u_k = \frac{1}{5}(-1 + 2i) = 5^{-1/2}e^{i\theta_k} \quad (4.6)$$

with

$$\theta_k = \pi - \arctan(2) \simeq 116.57^\circ \quad (4.7)$$

As in our earlier works [11, 12, 13], we denote these as multiple points, following the technical terminology of algebraic geometry, according to which a multiple point of an algebraic curve is a point where two or more branches (arcs) of the curve cross [21]. We shall use the words “intersection point” and “multiple point” synonymously here. The corresponding numerical values of $z_k = \pm 5^{-1/4}e^{i\theta_k/2}$ are

$$z_k = \pm(0.3515776 + 0.5688645i) \quad (4.8)$$

Finally, as x decreases from -1 toward $-3/2$, these split again, with one root moving away from u_k upward along an arc of the circle defined by

$$\left|u - \frac{1}{3}\right| = \frac{2}{3} \quad (4.9)$$

toward the endpoint of this arc on the positive imaginary axis, given by

$$u_e = \frac{i}{\sqrt{3}} \quad (4.10)$$

the conjugate root moving down from u_k^* on the circle (4.9) toward u_e^* , and the other two roots moving along the circle (4.9) toward the real axis. Finally, at $x = -3/2$, two roots occur at the endpoints u_e, u_e^* , and there is a double root at the point $u = u_\ell \equiv -1/3$.

In terms of the commonly used variable z , the complex phase diagram is shown in Fig. 5(b). From the fact that the equation (4.3) for the locus of points where f is non-analytic is symmetric under $z \rightarrow -z$, it follows that the phase diagram in the z plane has this symmetry also. The physical critical point is $z_c = (-1 + 2/\sqrt{3})^{1/2} \simeq 0.393320...$. The boundary of the complex-temperature FM phase crosses the real z axis at the points $\pm z_c$. Corresponding to

the intersection point u_k and its conjugate there are four intersection points $z_k = 5^{-1/4}e^{i\theta_k/2}$, $-z_k$, and $\pm z_k^*$. The outermost points on the boundaries of the O phases are given by $z_o = i|(-1 - 2/\sqrt{3})|^{1/2}$ and z_o^* .

Finally, by a conformal mapping or directly from eq. (4.1), one can also determine the corresponding loci of points in the v plane. The equation for this locus of points is

$$1 - 4v + 10v^2 - 16v^3 + 22v^4 - 16v^5 + 10v^6 - 4v^7 + v^8 - 2v^2(1-v)^2(1+v^2)x = 0 \quad (4.11)$$

Up to an overall factor of v^{-8} , this equation is invariant under the transformation $v \rightarrow 1/v$. This together with the reality of the coefficients implies that the locus of solutions is invariant under (i) $v \rightarrow v^*$ and (ii) $v \rightarrow 1/v$. This locus is shown in Fig. 5(c). The complex-temperature phases are marked on this figure and consist of the PM and FM phases, together with two O phases which are related to each other by complex conjugation. From the value of u_c or z_c and the relation (2.3), it follows that the critical value of v is

$$v_{c,kag.} = \frac{1}{2}(1 + 3^{1/2})[1 - (2\sqrt{3} - 3)^{1/2}] \simeq 0.43542054... \quad (4.12)$$

One sees that the kidney-shaped curve enclosing the FM and two O phases crosses the real- v axis at the points v_c and $1/v_c \simeq 2.29663...$. The four intersection points of the kidney-shaped curve and the arcs are given by $v_k = (1 - z_k)/(1 + z_k)$, its complex conjugate, v_k^* , and their two reciprocals, $1/v_k$ and $1/v_k^*$. Similarly, the four endpoints of the arcs are given by $v_e = (1 - z_e)/(1 + z_e)$, v_e^* , $1/v_e$, and $1/v_e^*$. We find that the inner endpoints of the arcs are the same distance from the origin as the physical critical point, i.e. $|v_e| = v_c$.

The phase structure consists of PM and FM phases, but, as is well known, no AFM phase because of the frustration associated with AFM ordering. These characteristics are the same as those for the (isotropic) Ising model on the triangular lattice. In addition, Figs. 5(a) and 5(b) show two complex-temperature phases denoted O and O* which have no overlap with any physical phase. In the u variable (see Fig. 5(c)), these are mapped onto a single O phase. In our previous work, we found O phases for the square and triangular (but not hexagonal) lattices, in the v and z plane. However, for both the square and triangular lattices, each point z in the O phase was just the negative of a corresponding point in the complex PM phase, and hence under the mapping from the z to u plane, these were mapped to the same point, which could be considered just the complex PM phase. We find for the kagomé lattice a new property, viz., a distinct O phase which persists even in the u plane.

The spontaneous magnetisation cannot be written in the same form $M = (1 - (k_{<,\Lambda})^2)^{1/8}$ as for the regular unipolygonal lattices $\Lambda = sq, tri, hc$. Rather, it has the following form in

the FM phase (and vanishes identically elsewhere) [22]

$$M_{kag.} = \frac{(1+3u)^{1/2}(1-u)^{1/2}}{(1+u)} \left(1 - (k_{<,kag.})^2\right)^{1/8} \quad (4.13)$$

where

$$k_{<,kag.} = \frac{2^{7/2}u^{3/2}(1+u)^{3/2}(1+3u^2)^{1/2}}{(1-u)^3(1+3u)} \quad (4.14)$$

i.e.,

$$M_{kag.} = \frac{(1-6u-3u^2)^{1/8}(1+2u+5u^2)^{3/8}(1+3u)^{1/4}}{(1-u)^{1/4}(1+u)} \quad (4.15)$$

These formulas may be analytically continued through the complex-temperature extension of the FM phase. Note the factorizations $1-6u-3u^2 = (1-u/u_{c,kag.})(1+3u_{c,kag.}u)$ and $1+2u+5u^2 = (1-u/u_k)(1-u/u_k^*)$.

From eq. (4.15) and our determination of the complex-temperature FM phase in which the analytic continuation of this formula holds, it follows that besides the well-known fact that $M_{kag.}$ vanishes continuously at the physical critical point u_c , with exponent $\beta = 1/8$, it also vanishes continuously at the complex-temperature points $u_\ell = -1/3$ with exponent

$$\beta_{kag.,\ell} = \frac{1}{4} \quad (4.16)$$

and at the points u_k and u_k^* with exponent

$$\beta_{kag.,k} = \frac{3}{8} \quad (4.17)$$

Elsewhere along the boundary of the complex-temperature FM phase, M vanishes discontinuously. One may observe that the expression for M has an apparent zero at $u = -1/(3u_{kag.,c}) = -1 - 2/\sqrt{3} \simeq -2.1547$ (the point where the left boundary in Fig. 5(a) crosses the real u axis) and apparent divergences at $u = 1$ and $u = -1$; however, none of these singularities actually occurs since all of these points are outside of the complex-temperature extension of the FM phase where the expression (4.15) holds. This is clear from the phase diagram in Fig. 5(a).

The characteristics of the points where M vanishes continuously are listed in Table 2, which includes a comparison with the three 2D homopolygonal lattices. The column marked z gives the symbol, if one was assigned, for each of the zeros (or divergences) in the uniform (and, where relevant, staggered) magnetisation. The column marked “value” lists either the analytic expression or, where this is too long to fit into the space, a reference to the equation(s) where this is given in the text. The column marked adj. phases lists the phases which are adjacent to the given point. For conciseness, some lines list a point and its complex

conjugate together; in these cases, the notation $O^{(*)}$ in the adjacent phase column means O for the first point and O^* for its complex conjugate. One may recall that the divergence in M for the triangular lattice occurs at $z = \pm 1/\sqrt{3}$ which are the endpoints of two line segments protruding into the complex-temperature FM phase; this is indicated in the table by the notation “protrusion in FM”. Other notation is explained in the table caption. It is also of interest to perform this comparison for the lattices with even coordination number, where all quantities can be expressed solely in terms of $u = z^2$; this is done in Table 3.

5 $(3 \cdot 12^2)$ Lattice

The (zero-field) free energy for the $(3 \cdot 12^2)$ lattice with isotropic couplings was given implicitly in [23, 17]. For various generalisations to unequal couplings, the free energy was given in Refs. [24] and [25]. Evaluating some intermediate expressions and performing some algebra, we obtain the explicit expression, in terms of z (and $K = -(1/2) \ln z$),

$$f_{3-12} = \frac{3}{2}K + \frac{1}{2} \ln(1+z) + \frac{1}{12} \int_{-\pi}^{\pi} \int_{-\pi}^{\pi} \frac{d\theta_1 d\theta_2}{(2\pi)^2} \ln[A_{3-12} + B_{3-12}P(\theta_1, \theta_2)] \quad (5.1)$$

where

$$A_{3-12} = 1 - 6z + 24z^2 - 42z^3 + 66z^4 - 42z^5 + 48z^6 - 6z^7 + 21z^8 \quad (5.2)$$

$$B_{3-12} = -2z(1-z+2z^2)(1+z)(1-z)^4 \quad (5.3)$$

Since this lattice has odd coordination number $q = 3$, Theorem 6 states that, in addition to the trivial singularities at $K = \pm\infty$, i.e., $z = 0, \infty$, the free energy f has a singularity at $z = -1$. This is evident in eq. (5.1). If one takes the branch cut for the logarithm to extend from $z = -1$ to $z = -\infty$, then as one approaches $z = -1$ from the direction of the origin, f becomes negatively infinite. In the case of the honeycomb lattice, as was noted in Ref. [13], this point lies on the continuous locus of points where the argument of the logarithm in the integrand analogous to (5.1) vanishes. However, in contrast to the honeycomb lattice, for the $(3 \cdot 12^2)$ and $(4 \cdot 8^2)$ lattices, this singularity is an isolated one. Aside from these isolated singular points, the free energy also has non-analyticities which arise from the vanishing of the argument of the logarithm inside of the integral in eq. (5.1). The condition for this vanishing is

$$A_{3-12} + B_{3-12}x = 0 \quad (5.4)$$

where x represents $P(\theta_1, \theta_2)$ as given above in eq. (4.2). This yields the curve shown in Fig. 6(a). As marked there, these curves serve to bound the complex-temperature extensions of

| Λ | z | value | M | M_{st} | β | adj. phases |
|-------------------------------|----------------------------|----------------------------|------|----------|---------|--|
| sq (4^4) | z_c | $\sqrt{2} - 1$ | zero | – | 1/8 | FM-PM |
| | $-z_c$ | $-(\sqrt{2} - 1)$ | zero | – | 1/8 | O-FM |
| | z_c^{-1} | $\sqrt{2} + 1$ | – | zero | 1/8 | PM-AFM |
| | $-z_c^{-1}$ | $-(\sqrt{2} + 1)$ | – | zero | 1/8 | AFM-O |
| | z_s, z_s^* | $\pm i$ | zero | zero | 1/4 | O-FM-PM-AFM (mp) |
| tri (3^6) | z_c | $1/\sqrt{3}$ | zero | N | 1/8 | FM-PM |
| | $-z_c$ | $-1/\sqrt{3}$ | zero | N | 1/8 | O-FM |
| | z_s, z_s^* | $\pm i$ | zero | N | 3/8 | O-PM-FM (mp) |
| | z_e, z_e^* | $\pm i/\sqrt{3}$ | div. | N | –1/8 | protrusion in FM |
| hex (6^3) | z_c | $2 - \sqrt{3}$ | zero | – | 1/8 | FM-PM |
| | z_c^{-1} | $2 + \sqrt{3}$ | – | zero | 1/8 | PM-AFM |
| | z_s, z_s^* | $\pm i$ | zero | zero | 3/8 | FM-PM-AFM (mp) |
| | | -1 | div. | div. | –1/4 | AFM-FM |
| $(3 \cdot 6 \cdot 3 \cdot 6)$ | z_c | $(-1 + 2/\sqrt{3})^{1/2}$ | zero | N | 1/8 | FM-PM |
| | $-z_c$ | $-(-1 + 2/\sqrt{3})^{1/2}$ | zero | N | 1/8 | PM-FM |
| | | $\pm i/\sqrt{3}$ | zero | N | 1/4 | FM-O, FM-O* |
| | $\pm z_k$ | eq. (4.8) | zero | N | 3/8 | FM-PM-O (mp) |
| | $\pm z_k^*$ | eq. (4.8) | zero | N | 3/8 | FM-PM-O* (mp) |
| $(3 \cdot 12^2)$ | $z_c = z_{a+}$ | eqs. (5.5),(5.6) | zero | N | 1/8 | FM-PM |
| | z_{a-} | eqs. (5.5),(5.7) | zero | N | 1/8 | PM-FM |
| | | $\pm i/\sqrt{3}$ | zero | N | 1/4 | FM-O ^(*) |
| | | $\pm i$ | zero | N | 3/8 | FM-PM-O ^(*) (mp) |
| | z_r, z_r^* | $(1 \pm 2i)/5$ | zero | N | 3/8 | FM-PM-O ^(*) (mp) |
| | | -1 | div. | N | –1/2 | interior of FM |
| $(4 \cdot 8^2)$ | $z_c = z_{1+}$ | eqs. (6.15),(6.20) | zero | – | 1/8 | FM-PM (mp;tn) |
| | $(z_{1-})^{-1}$ | eqs. (6.17),(6.21) | zero | – | 1/8 | O ₁ -FM (mp;tn) |
| | z_{3-}^*, z_{3-} | eqs. (6.19),(6.25) | zero | – | 1/8 | FM-O ₂ ^(*) (mp) |
| | $z_c^{-1} = (z_{1+})^{-1}$ | eqs. (6.17),(6.20) | – | zero | 1/8 | PM-AFM (mp;tn) |
| | z_{1-} | eqs. (6.15),(6.21) | – | zero | 1/8 | AFM-O ₁ (mp;tn) |
| | z_{3+}, z_{3+}^* | eqs. (6.19),(6.24) | – | zero | 1/8 | AFM-O ₃ ^(*) (mp) |

Table 2: Points at which M and M_{st} vanish continuously (or diverge) for the $(3 \cdot 6 \cdot 3 \cdot 6)$ (kagomé), $(3 \cdot 12^2)$, and $(4 \cdot 8^2)$ (bathroom tile) lattices, together with the three homopolygona 2D lattices, for comparison. Under the M and M_{st} columns, an entry marked – means that the point cannot be reached from within the FM and AFM phases, respectively. The symbol N means that the model has no AFM phase. (mp) means a multiple (=intersection) point through two or more phase boundary arcs. See text for further discussion.

| Λ | u | formula | value | M | M_{st} | β | adj. phases |
|-------------------------------|--------------|-------------------|-------|------|----------|---------|------------------|
| sq (4^4) | u_c | $3 - 2\sqrt{2}$ | 0.172 | zero | — | 1/8 | FM-PM |
| | u_c^{-1} | $3 + 2\sqrt{2}$ | 5.83 | — | zero | 1/8 | PM-AFM |
| | u_s | -1 | | zero | zero | 1/4 | AFM-FM-PM (mp) |
| tri (3^6) | u_c | 1/3 | | zero | N | 1/8 | FM-PM |
| | u_s | -1 | | zero | N | 3/8 | PM-FM (mp) |
| | u_e | -1/3 | | div. | N | -1/8 | protrusion in FM |
| $(3 \cdot 6 \cdot 3 \cdot 6)$ | u_c | $-1 + 2/\sqrt{3}$ | 0.155 | zero | N | 1/8 | FM-PM |
| | u_ℓ | -1/3 | | zero | N | 1/4 | O-FM |
| | u_k, u_k^* | $(-1 \pm 2i)/5$ | | zero | N | 3/8 | O-FM-PM (mp) |

Table 3: Points in the u plane at which M and M_{st} vanish continuously (or diverge) for the lattices with even coordination number q . Notation is the same as in Table 2.

the FM and PM phases and also two phases which have no overlap with any physical phase, and are labelled O and O*. The border of the complex FM phase crosses the real z axis at the points

$$z_{a\pm} = \frac{1}{2} \left[-(\sqrt{3} + 1) \pm \left(4 + \frac{10}{3} \sqrt{3} \right)^{1/2} \right] \quad (5.5)$$

with numerical values

$$z_{a+} = 0.19710468... \quad (5.6)$$

$$z_{a-} = -2.9291555... \quad (5.7)$$

The physical critical point of the model is $z_{c,3-12} = z_{a+}$. The intersection points nearest to the real z axis are given by z_r and z_r^* , where

$$z_r = \frac{1 - 2i}{5} = 5^{-1/2} e^{i\theta_k} \quad (5.8)$$

where θ_k was given above in eq. (4.7) (for certain formally analogous points in the u plane). The intersection points farther out from the real z axis occur at $z = \pm i$. For $x = 3$, there are four double roots at z_{a+} , z_{a-} , z_b , and z_b^* , where

$$\begin{aligned} z_b &= \frac{1}{2} \left[(\sqrt{3} - 1) + \left(4 - \frac{10}{3} \sqrt{3} \right)^{1/2} \right] \\ &\simeq 0.36602540 + 0.66586461i \end{aligned} \quad (5.9)$$

As can be seen from Fig. 6(a), the points z_b and z_b^* lie roughly at the centers of the outer boundaries of the respective O and O* phases. As x decreases from 3 in the range $-1 \leq x \leq 3$, these double roots split apart into pairs the members of which move away from these four points, tracing the curves shown in Fig. 6(a). At $x = -1$, these points rejoin at the four intersection points $z = \pm i$ and $z = z_r$ and z_r^* . As x decreases further in the range $-3/2 \leq x \leq -1$, these four double roots split again, with two of the roots moving toward each other on the arc forming the inner boundary of the O phase adjacent to the FM phase, and similarly with two other roots on the inner boundary of the O* phase, while the other four roots move outward away from the origin along the two arcs and their complex conjugates. Finally, at $x = -3/2$, two pairs of roots on the inner arcs join to form double roots at $z = \pm i/\sqrt{3}$, while the four outer roots reach the endpoints of the arcs. These endpoints are as follows:

$$z_{e\pm} = \frac{1}{2} \left[e^{i\pi/3} \pm \left(e^{2i\pi/3} - (4/3)\sqrt{3}e^{i\pi/6} \right)^{1/2} \right] \quad (5.10)$$

with the values

$$z_{e+} \simeq 0.29556791 - 0.3588689i \quad (5.11)$$

$$z_{e-} \simeq 0.20443209 + 1.2248943i \quad (5.12)$$

are, respectively, the endpoints of the upper parts of the arcs in the upper and lower half z plane. Their complex conjugates z_{e+}^* and z_{e-}^* form the endpoints of the lower parts of these arcs.

From implicit expressions given in Ref. [24], we can express the spontaneous magnetisation as

$$M_{3-12} = \frac{(1 - 6z + 6z^2 - 6z^3 - 3z^4)^{1/8} (1 + 3z^2)^{1/4} (1 + z^2)^{3/8} (1 - 2z + 5z^2)^{3/8}}{(1 - z)(1 + z)^{1/2}(1 - z + 2z^2)} \quad (5.13)$$

By analytic continuation, this expression holds throughout the complex-temperature extension of the FM phase, which we have determined, as shown in Fig. 6(a). Note the factorization

$$1 - 6z + 6z^2 - 6z^3 - 3z^4 = -3(z - z_{a+})(z - z_{a-})(z - z_b)(z - z_b^*) \quad (5.14)$$

Moreover, similar to another formula above (for u rather than z), we have the factorization $1 - 2z + 5z^2 = (1 - z/z_r)(1 - z/z_r^*)$. Finally, we note that $1 - z + 2z^2 = 2(z - z_o)(z - z_o^*)$, where

$$z_o = \frac{1}{4}(1 + i\sqrt{7}) = 0.25 + i0.66143783... \quad (5.15)$$

These points z_o and z_o^* lie in the middle of the two complex conjugate O phases. Thus, M_{3-12} vanishes continuously at the eight points z_{a+} , z_{a-} , $\pm i/\sqrt{3}$, $\pm i$, z_r , and z_r^* . In Table 2 we list these zeros, together with the corresponding exponents β and the phases which are adjacent at each point. Elsewhere along the boundary of the complex-temperature FM phase, M vanishes discontinuously. M_{3-12} also has a divergence at the isolated point $z = -1$ in the interior of the complex-temperature FM phase, where the free energy itself is also singular. In addition to these actual singularities, the formal expression (5.13) has apparent zeros at the points z_{b+} , $z_{b-} = z_{b+}^*$, z_o , and z_o^* , but these are not zeros of the actual magnetisation, since these points cannot be reached from within the complex-temperature FM phase where the expression (5.13) holds. As one can see from Fig. 6(a), z_b lies on the boundary separating the O and PM phase, and similarly z_b^* lies on the boundary between the O* and PM phase. The points z_o and z_o^* lie in the interior of the O and O* phases, respectively.

6 $(4 \cdot 8^2)$ Lattice

In contrast to the $(3 \cdot 6 \cdot 3 \cdot 6)$ and $(3 \cdot 12^2)$ lattices, the $(4 \cdot 8^2)$ (bathroom tile) lattice is bipartite, and the physical phase diagram consists of a PM, FM, and also AFM phase. One way to obtain the (zero-field) free energy is from the free energy for the dual $[4 \cdot 8^2]$ (union jack) lattice. An explicit calculation of the latter for the case of equal spin-spin couplings was given in [26]. (See also the remarks in Ref. [16]; for the union jack lattice with general couplings, which we shall not need here, see also Refs. [27] and [28].) Using this duality relation, one easily obtains the free energy for the $(4 \cdot 8^2)$ lattice, in terms of z (and $K = -(1/2) \ln z$), as follows:

$$f_{4-8} = \frac{3}{2}K + \frac{1}{2} \ln(1+z) + \frac{1}{8} \int_{-\pi}^{\pi} \int_{-\pi}^{\pi} \frac{d\theta_1 d\theta_2}{(2\pi)^2} \ln \left[A_{4-8}(z) + B_{1;4-8}(z)(\cos \theta_1 + \cos \theta_2) + B_{2;4-8}(z) \cos \theta_1 \cos \theta_2 \right] \quad (6.1)$$

where

$$A_{4-8}(z) = (1+z^2)^2(1-4z+10z^2-4z^3+z^4) \quad (6.2)$$

$$B_{1;4-8}(z) = 2z(1-z)^3(1+z)(1+z^2) \quad (6.3)$$

$$B_{2;4-8}(z) = -4z^2(1-z)^4 \quad (6.4)$$

In addition to the trivial singularities at $K = \pm\infty$, i.e., $z = 0, \infty$, and the additional isolated singularity at $z = -1$, the free energy has non-analyticities where the argument of the

logarithm in the integrand of eq. (6.1) vanishes. These are given by the equation

$$A_{4-8}(z) + B_{1;4-8}(z)(\cos \theta_1 + \cos \theta_2) + B_{2;4-8}(z) \cos \theta_1 \cos \theta_2 = 0 \quad (6.5)$$

We find that the locus of points which are solutions to this equation fall, in general, into areas rather than curves, in the z or, equivalently, the v planes. These areas degenerate into points at certain special locations. In Fig. 7(a) we show the solution to eq. (6.5) in the z plane, for a grid of values of θ_1 and θ_2 . Because of the finite grid of values of θ_1 and θ_2 used to make the plots, the zeros show a striped structure in certain regions; it is understood that in the limit where the aforementioned grid of values of θ_1 and θ_2 becomes infinitely fine, these stripes would merge into coherent areas; the boundaries of these areas are easily inferred from the plot. The phases include the complex-temperature extensions of the physical FM, PM, and AFM phases, as marked, together with five phases which have no overlap with any physical phases, labelled O_1 , O_2 , O_2^* , O_3 , and O_3^* . The rest of the z plane involves various continuous regions of points where the free energy is non-analytic (forming the thermodynamic limits of zeros of the partition functions for finite lattices). We shall discuss the special locations where the areas of zeros of the partition function degenerate into points below, in conjunction with an analysis of the spontaneous uniform and staggered magnetisations. The corresponding diagram in the v plane is shown in Fig. 7(b). As in Fig. 7(a), because of the finite grid of values of θ_1 and θ_2 used to make the plot, the zeros exhibit a striped or dotted structure in certain regions; again, it is understood that for a dense set of values of θ_1 and θ_2 , the zeros in these regions form a continuous set.

To our knowledge, this finding constitutes the first known case of an Ising model with isotropic spin-spin couplings, where the non-analyticities of the free energy (aside from the trivial ones at $K = \pm\infty$ and, for odd q , at $z = -1$, as proved in Theorem 6) form a two-dimensional, rather than one-dimensional, algebraic variety, i.e., lie in areas rather than on curves (including line segments). It is easy to understand the basis for this result. The locus of points at which the free energy is non-analytic (aside from the above-mentioned trivial singularities) is determined by the condition that in the integral occurring in the free energy, the expression in the argument of the logarithm vanishes. For homopolygonal lattices, this expression reduces to the equation

$$A_\Lambda(z) + B_\Lambda(z)x = 0 \quad (6.6)$$

for isotropic spin-spin couplings, where x represents the function $P(\theta_1, \theta_2) = \cos \theta_1 + \cos \theta_2$ for the square lattice and $P(\theta_1, \theta_2) = \cos \theta_1 + \cos \theta_2 + \cos(\theta_1 + \theta_2)$ for the triangular and hexagonal (honeycomb) lattices. (Thus for the square lattice, $-2 \leq x \leq 2$, while for the

triangular and hexagonal lattices, $-3/2 \leq x \leq 3$.) The solutions to eq. (6.6) form a one-dimensional algebraic variety, specifically, algebraic curves (including possible line segments). In contrast, for unequal spin-spin exchange constants J_i , where $i = 1, 2$ for the square lattice, and $i = 1, 2, 3$ for the triangular and hexagonal lattices, the condition for the argument of the logarithm in the integrand to vanish is of the form

$$A_{sq} + B_{sq;1} \cos \theta_1 + B_{sq;2} \cos \theta_2 = 0 \quad (6.7)$$

for the square lattice, and

$$A_{\Lambda} + B_{\Lambda;1} \cos \theta_1 + B_{\Lambda;2} \cos \theta_2 + B_{\Lambda;3} \cos(\theta_1 + \theta_2) = 0 \quad (6.8)$$

for the triangular and hexagonal lattices, where in each case, the various A and B functions depend on the z_i , with $z_i = e^{-2K_i}$ and $K_i = \beta J_i$. Now let the (anisotropic) ratios of the J_i 's be fixed. Then eqs. (6.7) and (6.8) depend on two independent real (periodic) variables, θ_1 and θ_2 . It follows that the solutions, in general, form a two-dimensional algebraic variety, specifically areas (which may degenerate to points at special values of z).

The heteropolygonal lattices $(3 \cdot 6 \cdot 3 \cdot 6)$ and $(3 \cdot 12^2)$ are similar to the homopolygonal lattices in this respect, i.e., if the spin-spin couplings on each link are equal, then the condition for the argument of the logarithm in the integrand to vanish is of the form (6.6). However, as is evident from eq. (6.1), this is not the case for the $(4 \cdot 8^2)$ lattice. That is, even if the spin-spin couplings are equal for each link, the condition for the vanishing of the argument of the logarithm in eq. (6.1) is of the form (6.5), which depends on two independent real (periodic) variables θ_1 and θ_2 .

The expression for the spontaneous magnetisation was conjectured by Lin et al. [29] and proved by Baxter and Choy [27]. As with the other heteropolygonal lattices Λ , M can be written (where it is nonzero) as a prefactor times $(1 - (k_{<,\Lambda})^2)^{1/8}$. Let us define (using the subscript $4 - 8$ to denote $(4 \cdot 8^2)$)

$$k_{<,(4-8)} = \frac{8z^2(1 - 2z + 4z^2 - 2z^3 + z^4)}{(1 - z)^4(1 + z^2)^2} \quad (6.9)$$

and

$$a = \frac{(1 + z^2)}{(1 + z)^{1/2}(1 - z + 3z^2 + z^3)^{1/2}} \quad (6.10)$$

Then $M_{4-8} = a(1 - (k_{<})^2)^{1/8}$, i.e.,

$$M_{4-8} = \frac{(1 - 4z - z^4)^{1/8}(1 + 4z^3 - z^4)^{1/8}(1 + z^2)^{1/2}(1 - 2z + 6z^2 - 2z^3 + z^4)^{1/4}}{(1 - z)(1 + z)^{1/2}(1 - z + 3z^2 + z^3)^{1/2}} \quad (6.11)$$

within the physical FM phase and, by analytic continuation, throughout the complex-temperature extension of the FM phase; M_{4-8} vanishes identically elsewhere. We observe first that under the transformation $z \rightarrow 1/z$, the numerator of this expression goes into itself times a power of z . It follows that the set of formal zeros of this numerator is invariant under the mapping $z \rightarrow 1/z$. In particular, under this mapping, the first and second quartic expressions in the numerator of M_{4-8} are interchanged, up to an overall power of z : $z \rightarrow 1/z \Rightarrow (1-4z-z^4) \rightarrow -z^{-4}(1+4z^3-z^4)$. The roots of these two quartics are therefore reciprocals of each other. Under this mapping, the other two factors, $(1+z^2)$ and $(1-2z+6z^2-2z^3+z^4)$ transform into themselves, up to overall powers of z , and consequently, their zeros also come in reciprocal pairs (since, furthermore they do not have either of the self-reciprocal numbers $z = \pm 1$ as roots). We note the factorizations

$$1 - 4z - z^4 = \left[1 - \sqrt{2}(\sqrt{2} + 1)z - (\sqrt{2} + 1)z^2\right] \left[1 - \sqrt{2}(\sqrt{2} - 1)z + (\sqrt{2} - 1)z^2\right] \quad (6.12)$$

$$1 + 4z^3 - z^4 = \left[1 + \sqrt{2}z - (\sqrt{2} - 1)z^2\right] \left[1 - \sqrt{2}z + (\sqrt{2} + 1)z^2\right] \quad (6.13)$$

$$1 - 2z + 6z^2 - 2z^3 + z^4 = \left[1 - 2e^{i\pi/3}z + z^2\right] \left[1 - 2e^{-i\pi/3}z + z^2\right] \quad (6.14)$$

The expression (6.12) has zeros at

$$z_{1\pm} = -\frac{1}{2} \left[\sqrt{2} \pm (-2 + 4\sqrt{2})^{1/2} \right] \quad (6.15)$$

$$z_{2\pm} = \frac{1}{2} \left[\sqrt{2} \pm i(2 + 4\sqrt{2})^{1/2} \right] \quad (6.16)$$

while the expression (6.13) has zeros at

$$(z_{1\pm})^{-1} = \frac{1}{2} \left[2 + \sqrt{2} \pm (10 + 8\sqrt{2})^{1/2} \right] \quad (6.17)$$

$$(z_{2\mp})^{-1} = \frac{1}{2} \left[2 - \sqrt{2} \pm (10 - 8\sqrt{2})^{1/2} \right] \quad (6.18)$$

The expression (6.14) has zeros at $z_{3\pm}$ and $z_{3\pm}^*$, where

$$z_{3\pm} = e^{i\pi/3} \pm (e^{2i\pi/3} - 1)^{1/2} \quad (6.19)$$

Note that $z_{3-} = z_{3+}^{-1}$. These roots have the approximate numerical values

$$z_{1+} = 0.2490384, \quad (z_{1+})^{-1} = 4.0154454 \quad (6.20)$$

$$z_{1-} = -1.663252, \quad (z_{1-})^{-1} = -0.60123183 \quad (6.21)$$

$$z_{2\pm} = 0.7071068 \pm 1.383551i \quad (6.22)$$

$$(z_{2\mp})^{-1} = 0.2928932 \pm 0.5730856i \quad (6.23)$$

$$z_{3+} = 0.8406250 + 2.137255i \quad (6.24)$$

$$z_{3-} = (z_{3+})^{-1} = 0.1593750 - 0.4052045i \quad (6.25)$$

Only a subset of these formal zeros are zeros of the actual magnetisation, namely those which can be reached from within the complex-temperature FM phase (they lie on the border of this phase) where the formula (6.11) holds; the other zeros are spurious, since they occur at points which cannot be reached in this manner, where consequently the formula does not apply. The true zeros of M are at $z_c = z_{1+}$, $1/z_{1-}$, z_{3-}^* , and z_{3-} . The first two of these are, respectively, the physical critical point and the point at which the left boundary of the complex-temperature FM phase crosses the real z axis. As one can see from Fig. 7(a), z_{3-}^* lies where certain areas of zeros of the partition function degenerate to a single point separating the complex-temperature FM and O_2 phases, and similarly for the complex conjugate point z_{3-} separating the FM and O_2^* phases. Indeed, these four points are precisely the full set of points on the border of the complex-temperature FM phase where various areas of zeros degenerate to single points. The exponents with which M_{4-8} vanishes continuously at these zeros are all equal to $1/8$. As one moves upward, away from the origin along the $Im(z)$ (vertical) axis in Fig. 7(a), one encounters a boundary followed by a dense set of points where the free energy is non-analytic before one reaches the point $z = i$. This boundary prevents analytic continuation, so that the zero at $z = i$, and similarly, the zero at $z = -i$, in the expression (6.11) are not true zeros of M . Note that the points $\pm i$ lie where the O_1 and PM phases are directly adjacent, and separated by these points. Similarly, all of the remaining zeros in the numerator of the expression (6.11) are not actual zeros of M . However, it is of some interest to observe where these spurious zeros lie. The point z_{2+} is located where the border between the O_3 and PM phases narrows to zero thickness (elsewhere this border is comprised of arcs forming strips, as one can see from Fig. 7(a)). An analogous comment applies, *mutatis mutandis*, for the complex conjugate point z_{2+}^* and the border between the O_3^* and PM phase. The reciprocal point $1/z_{2-}$ is located where the border between the O_2 and PM phase narrows to zero thickness, and similarly for the point $1/z_{2+}^*$ and the border between the O_2^* and PM phases. The point z_{3+} lies where two areas of zeros of the partition function degenerate to a point separating the O_3 and AFM phases, and similarly for z_{3+}^* and the border between the O_3^* and AFM phases. Finally, none of the the apparent divergences in M_{4-8} actually occurs; $z = 1$ lies in the interior of the PM phase; $z = -1$ is in the interior of the O_1 phase, and among the roots of the cubic $1 - z + 3z^2 + z^3$, $z \simeq -3.38$ is in the AFM phase, while $z \simeq 0.191 \pm 0.509i$ lie in the interiors of the O_2 and O_2^* phases, respectively. In the case of the point $z = -1$, it is interesting to compare this with the situation for the

$(3 \cdot 12^2)$ lattice. In both cases, since q is odd, f is singular at $z = -1$. For the $(3 \cdot 12^2)$ lattice, this point lies within the complex-temperature extension of the FM phase, and M is also singular (divergent) at this point. In contrast, for the $(4 \cdot 8^2)$ lattice, this point is not within the complex-temperature FM phase, but rather in the interior of one of the O phases, and hence there is no associated singularity in M at this point.

As with other bipartite lattices, the staggered spontaneous magnetisation $M_{st,4-8}$ is given by eq. (3.8) in terms of M_{4-8} in the complex-temperature extension of the AFM phase and vanishes elsewhere. We may thus read off the zeros of $M_{st,4-8}$ immediately; these are precisely the inverses of the four zeros of M , i.e., z_c^{-1} , z_{1-} , $(z_{3-})^{-1} = z_{3+}$, and $(z_{3-}^*)^{-1} = z_{3+}^*$. The first point is the physical critical point separating the PM and AFM phase. The second is the point where the boundary between the AFM and O phases crosses the negative real z axis. The third is where the border between the O_3 and AFM phases narrows to zero thickness, and similarly for the fourth point, separating the O_3^* and AFM phases. The actual zeros of M and M_{st} are listed in Table 2.

In Table 4 we compare the general properties of the complex-temperature phase diagrams for the Ising model on homopolygonal and heteropolygonal 2D Archimedean lattices, in terms of the variable z , or equivalently, v . Since we have already indicated in Table 2 which lattices have AFM phases, and since all have PM and FM phases, we do not include that information here. The entries in the column marked N_O are the number of O phases. We observe that the Ising model on heteropolygonal lattices exhibits more of these O phases than on homopolygonal lattices. As we have discussed in our earlier papers [11, 12, 13], the points at which the curves (or line segments, if present) cross are singular points of the algebraic curves, in the technical terminology of algebraic geometry [21]. This usage of the term should, of course, not be confused with the different meaning of “singular point” in statistical mechanics; for example, the point $z_c = (-1 + 2/\sqrt{3})^{1/2}$ of the Ising model on the kagomé lattice is a singular point (actually, the physical critical point separating the PM and FM phases) in the statistical mechanical sense, but is not a singular point of the curve forming the outer boundary of the complex-temperature FM phase, in the algebraic geometry sense (see Fig. 5(b)). A singular point of the algebraic curve is denoted as a multiple point of index n_b if n_b branches (arcs) of the curve pass through the point. (We use the terms “multiple point” and “intersection point” synonymously here.) In the column marked “mult. pt.”, we list information about these multiple points, including the number and the index. The symbol *cc* means that the multiple points occur in complex conjugate pairs, while “real” means that the multiple points occur on the real axis in the z (equivalently, v) plane. For a normal double point, i.e., a multiple point of index 2, one may assign an

angle θ_{cr} as the angle between the tangents of the two branches (arcs) of the curve which pass through the point. All three homopolygonal lattices have multiple points on the curves (including line segments) across which the free energy is non-analytic. Each of these multiple points has index 2 and $\theta_{cr} = \pi/2$, i.e., the two branches cross in an orthogonal manner. Our results as shown in Figs. 5 and 6 show that the multiple points for the $(3 \cdot 6 \cdot 3 \cdot 6)$ and $(3 \cdot 12^2)$ lattices also have index 2 and $\theta_{cr} = \pi/2$. Note that because the transformation (2.3) relating z and v and also the transformation $u = z^2$ are conformal mappings, they preserve angles, so that a given θ_{cr} is the same for a multiple point in the z , v , and u plane. For all of these four lattices, the multiple points occur as complex conjugate pairs as functions of z . A general observation is that the heteropolygonal lattices have more multiple points on their curves than the homopolygonal lattices. The situation with the $(4 \cdot 8^2)$ lattice is the most complicated, since in this case the loci of points where the free energy is non-analytic form areas instead of curves. As one can see from Fig. 7, there are a number of multiple points through which more than one of the boundaries of these areas pass. There are 18 such points in all; of these, 14 consist of complex conjugate pairs while the remaining four lie on the real z or v axis. Of the 14 complex conjugate multiple points, 12 have index $n_b = 2$ (with various values of crossing angles θ_{cr}). The four multiple points lying on the real axis (namely, $z_c = z_{1+}$, $1/z_c$, z_{1-} , and $1/z_{1-}$) have index $n_b = 2$ and $\theta_{cr} = 0$. In the terminology of algebraic geometry, they are therefore (simple) tacnodes. We recall that a (simple) tacnode is defined as a multiple point of an algebraic curve through which two branches pass, in an osculating manner, i.e. such that their tangents coincide where the branches touch, so that $n_b = 2$ but the number of distinct tangents at the point is $n_t = 1$ [21]. We have denoted this in Tables 2 and 4 by the notation “tn”, standing for “tacnode”. A generalised tacnode is a multiple point of an algebraic curve for which some of the tangents of the branches passing through the point coincide, so that $n_b > n_t$ (and n_b may be greater than 2). The $(4 \cdot 8^2)$ lattice is the first one which we have studied which exhibits tacnodal points on the loci of points where the free energy is non-analytic. We come next to the multiple points at $\pm i$. These are, again, of a type unprecedented in any of the cases which we have previously studied; they have index 4 and are the first example of a multiple point of index higher than 2. Of the 4 branches which pass through this point, two cross at an angle of $\pi/2$ with respect to each other, the northeast – southwest and northwest – southeast curves), while two others pass through the points in a north – south direction, hence with a crossing angle of $\pi/4$ with respect to the former two curves and a crossing angle of 0 with respect to each other. This multiple point is therefore a higher-order tacnodal point, with $n_b = 4$ and $n_t = 3$. Finally, in the last column of Table 4 we list the number of endpoints of the algebraic curves and in which complex-temperature phase these endpoints lie. For all cases, the endpoints occur in

| lattice | N_O | mult. pt. | endpt. |
|-------------------------------|-------|--------------------------|--------------|
| sq (4^4) | 1 | 2: 2, cc | 0 |
| tri (3^6) | 1 | 2: 2, cc | 2, cc, in FM |
| hex (6^3) | 0 | 2: 2, cc | 2, cc, in PM |
| $(3 \cdot 6 \cdot 3 \cdot 6)$ | 2 | 4: 2, cc | 4, cc, in PM |
| $(3 \cdot 12^2)$ | 2 | 4: 2, cc | 4, cc, in PM |
| $(4 \cdot 8^2)$ | 3 | 18; see below: | 0 |
| | | 12: 2, cc | |
| | | 2: 3, cc, tn ($\pm i$) | |
| | | 4: 2, real, tn | |

Table 4: Comparison of some properties of complex-temperature phase diagrams, as functions of z or equivalently v , for the Ising model on homopolygonal and heteropolygonal Archimedean lattices. N_O denotes the number of O phases. In column marked “mult. pt.”, the entry 2: 2, cc means that there are 2 multiple points, each of index 2, and they occur as complex conjugate pairs, etc. for other entries. The notation “tn” means a tacnodal multiple point. For the $(4 \cdot 8^2)$ lattice we have listed the properties of the various types of multiple points underneath the general number, 18. See text for further discussion.

complex conjugate pairs.

For lattices with even q , viz., the square, hexagonal, and kagomé lattices, a more compact way to present the complex-temperature phase diagrams is in the u plane. In Table 5 we list the analogous characteristics for these lattices.

7 Conclusions

In this paper, using exact results, we have determined the complex-temperature phase diagrams and singularities of the spontaneous magnetisation on three heteropolygonal Archimedean lattices, $(3 \cdot 6 \cdot 3 \cdot 6)$ (kagomé), $(3 \cdot 12^2)$, and $(4 \cdot 8^2)$ (bathroom tile). This study reveals a rich variety of complex-temperature singularities and provides an interesting comparison with the situation for the three homopolygonal lattices. In particular, we have found the first example of a lattice where, even for equal spin-spin exchange couplings, the nontrivial non-analyticities of the free energy lie in areas rather than on curves, in the z (or equivalently, v) plane. We have also given a simple explanation of why this happens.

This research was supported in part by the NSF grant PHY-93-09888.

| lattice | N_O | mult. pt. | endpt. |
|---------------------------------|-------|------------|----------------|
| sq (4^4) | 0 | 1: 2, real | 0 |
| tri (3^6) | 0 | 1: 2, real | 1, real, in FM |
| ($3 \cdot 6 \cdot 3 \cdot 6$) | 1 | 2: 2, cc | 2, cc, in PM |

Table 5: Comparison of some properties of complex-temperature phase diagrams, as functions of u , for the Ising model on lattices with even coordination number q . Notation is as in Table 4.

References

- [1] Onsager, L. 1944 *Phys. Rev.* **65** 117.
- [2] Yang, C. N. 1952 *Phys. Rev.* **85** 808.
- [3] Domb, C. 1960 *Adv. in Phys.* **9** 149.
- [4] Fisher, M. E. 1965 *Lectures in Theoretical Physics* (Univ. of Colorado Press, Boulder), vol. 12C, p. 1.
- [5] Thompson, C. J., Guttmann, A. J., Ninham, B. W. 1969 *J. Phys. C* **2** 1889; Guttmann, A. J. 1969 *ibid*, 1900.
- [6] Domb, C. and Guttmann, A. J. 1970 *J. Phys. C* **3** 1652.
- [7] Guttmann, A. J. 1975 *J. Phys. A: Math. Gen.* **8** 1236.
- [8] Itzykson, C., Pearson, R., and Zuber, J.B. 1983 *Nucl. Phys. B* **220** 415.
- [9] Marchesini, G. and Shrock, R. E. 1989 *Nucl. Phys. B* **318** 541.
- [10] Enting, I. G., Guttmann, A. J., and Jensen, I. 1994 *J. Phys. A: Math. Gen.* **27** 6963.
- [11] Matveev, V. and Shrock, R., “Complex-Temperature Singularities of the Susceptibility in the $d = 2$ Ising Model. I. Square Lattice” (Aug. 1994) (hep-lat/9408020), *J. Phys. A: Math. Gen.*, in press.
- [12] Matveev, V. and Shrock, R., “Complex-Temperature Singularities in the $d = 2$ Ising Model. II. Triangular Lattice” ITP-SB-94-53 (Nov. 1994) (hep-lat/9411023).

- [13] Matveev, V. and Shrock, R., “Complex-Temperature Singularities in the $d = 2$ Ising Model. III. Honeycomb Lattice”, ITP-SB-94-54 (Dec. 1994) (hep-lat/9412076).
- [14] Matveev, V. and Shrock, R., “Complex-Temperature Properties of the 2D Ising Model with $\beta H = i\pi/2$ ”, ITP-SB-94-57 (Dec. 1994) (hep-lat/9412105).
- [15] Grünbaum, B. and Shephard, G. 1989 *Tilings and Patterns: an Introduction* (Freeman, 1989).
- [16] Utiyama, T. 1951 *Prog. Theor. Phys.* **6** 907.
- [17] Syozi, I. 1972 in *Phase Transitions and Critical Phenomena*, Domb, C. and Green, M. S., eds. (Wiley, New York), v. 1, p. 269.
- [18] Laves, F. 1930 *Zeitschrift für Kristallographie* **73** 202; Laves, F. 1931 *ibid.* **78** 208.
- [19] van Saarloos, W. and Kurtze, D. 1984 *J. Phys. A: Math. Gen.* **17** 1301; Stephenson, J. and Couzens, R. 1984 *Physica* **129A** 201; Wood, D. 1985 *J. Phys. A: Math. Gen.* **18** L481; Stephenson, J. 1986 *Physica* **136A** 147; Stephenson, J. and van Aalst, J. 1986 *ibid.* **136A** 160; Stephenson, J. 1988 *ibid.* **148A** 88, 107.
- [20] Kano, K. and Naya, S. 1953 *Prog. Theor. Phys.* **10** 158.
- [21] Lefschetz, S. 1953 *Algebraic Geometry* (Princeton Univ. Press, Princeton); Hartshorne, R. 1977 *Algebraic Geometry* (Springer, New York).
- [22] Naya, S. 1954 *Prog. Theor. Phys.* **11** 53.
- [23] Syozi, I. 1955 *Rev. Kobe Univ. Mercantile Marine* **2** 21.
- [24] Huckaby, D. 1986 *J. Phys. C: Solid State Phys.* **19** 5477.
- [25] Lin, K. Y. and Chen, J. L. 1987 *J. Phys. A: Math. Gen.* **20** 5695.
- [26] Vaks, V. G., Larkin, A. I., and Ovchinnikov, Yu. N. 1966 *JETP* **22** 820 (*Zh. Ek. Teor. Fiz.* **49** 1180).
- [27] Baxter, R. J. and Choy, T. C. 1988 *J. Phys. A: Math. Gen.* **21** 2143.
- [28] Wu, F. Y. and Lin, K. Y. 1987 *J. Phys. A: Math. Gen.* **20** 5737.
- [29] Lin, K. Y., Kao, C. H., and Chen, T. L. 1987 *Phys. Lett. A* **121** 443.

[30] Syozi, I. and Naya, S. 1960 *Prog. Theor. Phys.* **23** 374; *ibid.* **24** 829.

[31] Baxter, R. J. 1986 *Proc. Roy. Soc. Lond.* **A404** 1.

Figure Captions

Fig. 1. The $(3 \cdot 6 \cdot 3 \cdot 6)$ (kagomé) lattice.

Fig. 2. The $(3 \cdot 12^2)$ lattice.

Fig. 3. The $(4 \cdot 8^2)$ (bathroom tile lattice).

Fig. 4. The $[4 \cdot 8^2]$ (union jack) lattice, which is the Laves lattice dual to the Archimedean lattice $(4 \cdot 8^2)$.

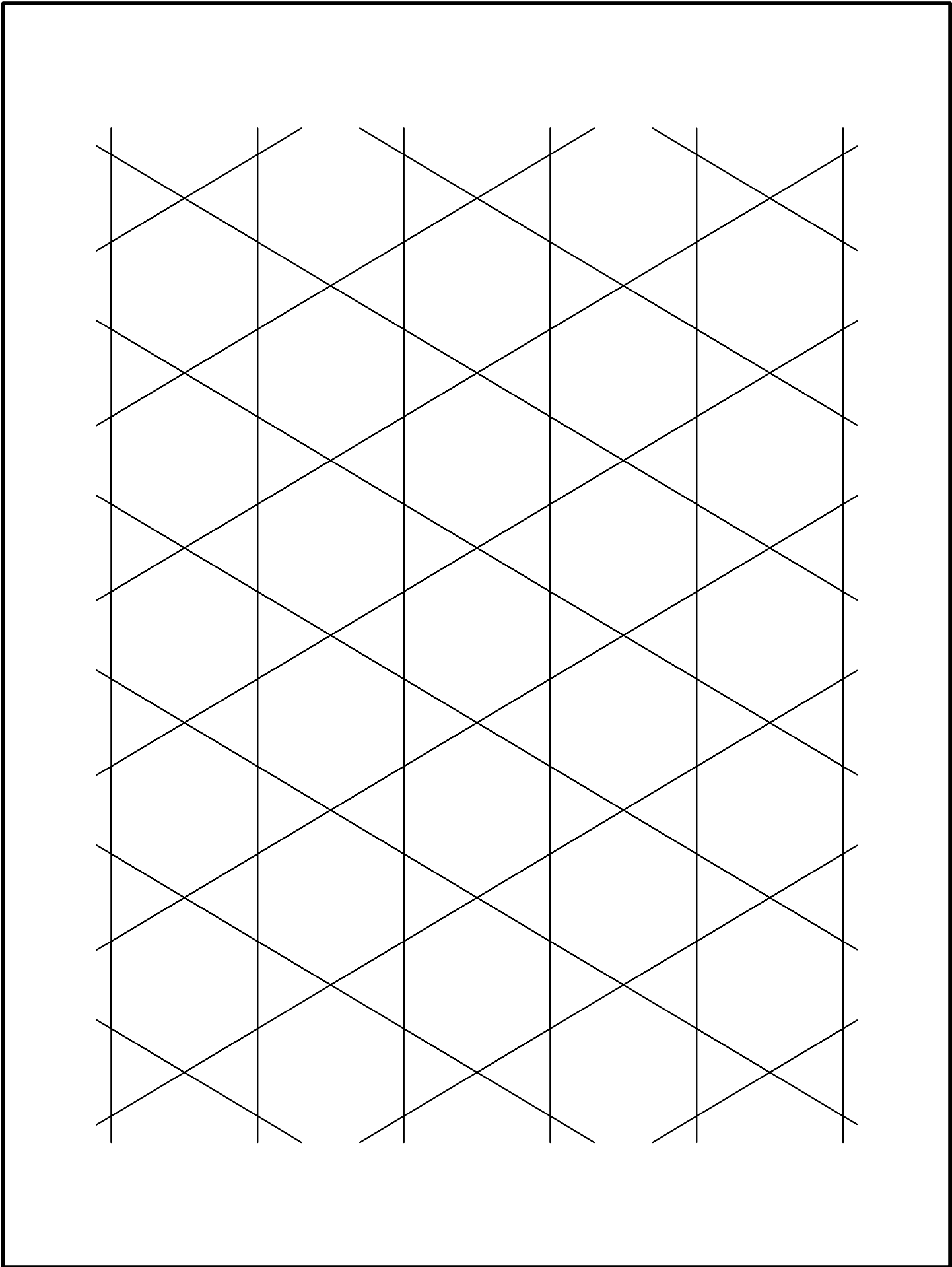
Fig. 5. Complex-temperature phase diagram for the Ising model on the $3 \cdot 6 \cdot 3 \cdot 6$ (kagomé) lattice, in the variable (a) u (b) z (c) v .

Fig. 6. Complex-temperature phase diagram for the Ising model on the $3 \cdot 12^2$ lattice, in the variable (a) z (b) v .

Fig. 7. Complex-temperature phase diagram for the Ising model on the $4 \cdot 8^2$ (bathroom tile) lattice, in the variable (a) z (b) v .

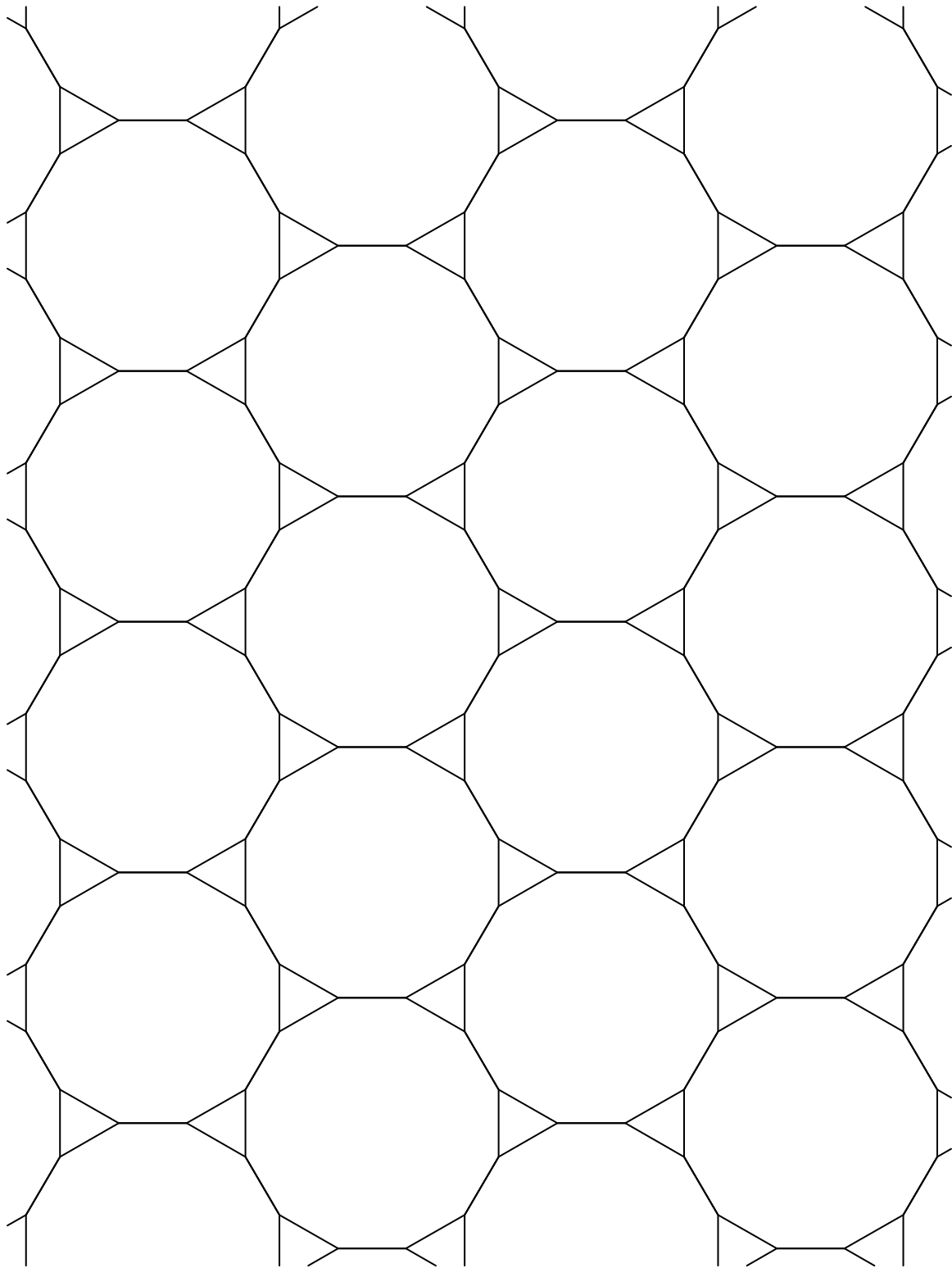
This figure "fig1-1.png" is available in "png" format from:

<http://arxiv.org/ps/hep-lat/9503005v1>



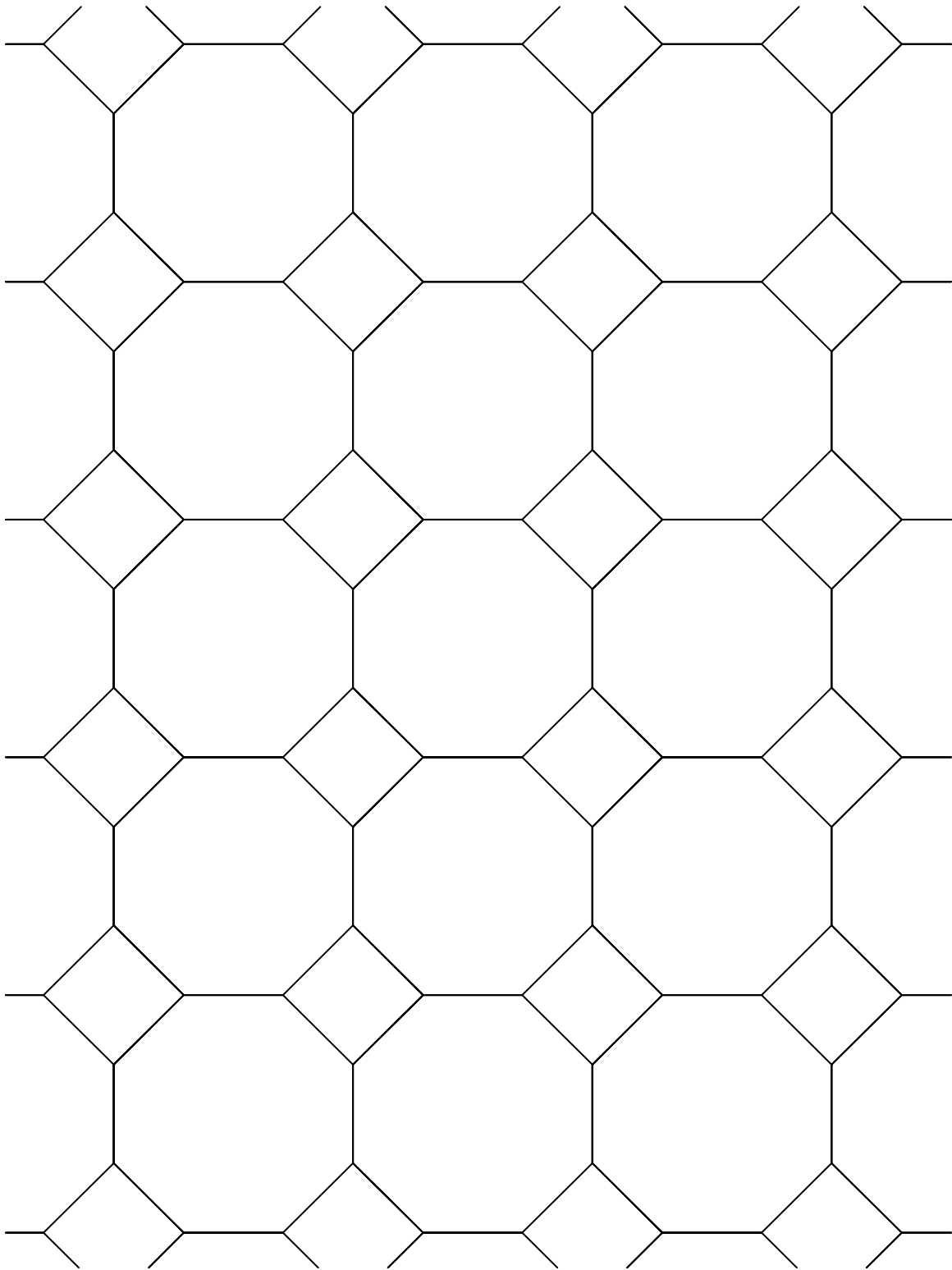
This figure "fig1-2.png" is available in "png" format from:

<http://arxiv.org/ps/hep-lat/9503005v1>



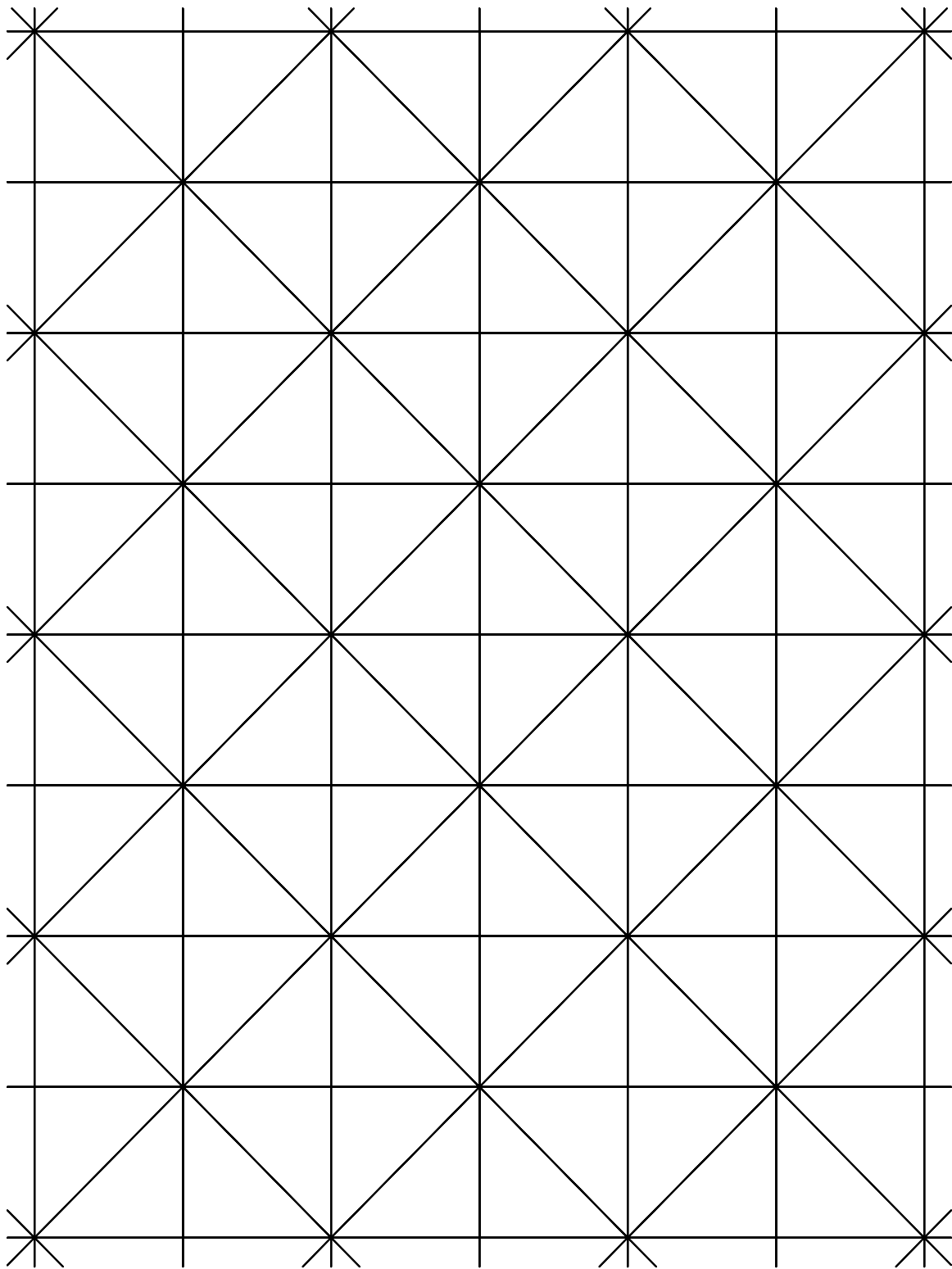
This figure "fig1-3.png" is available in "png" format from:

<http://arxiv.org/ps/hep-lat/9503005v1>



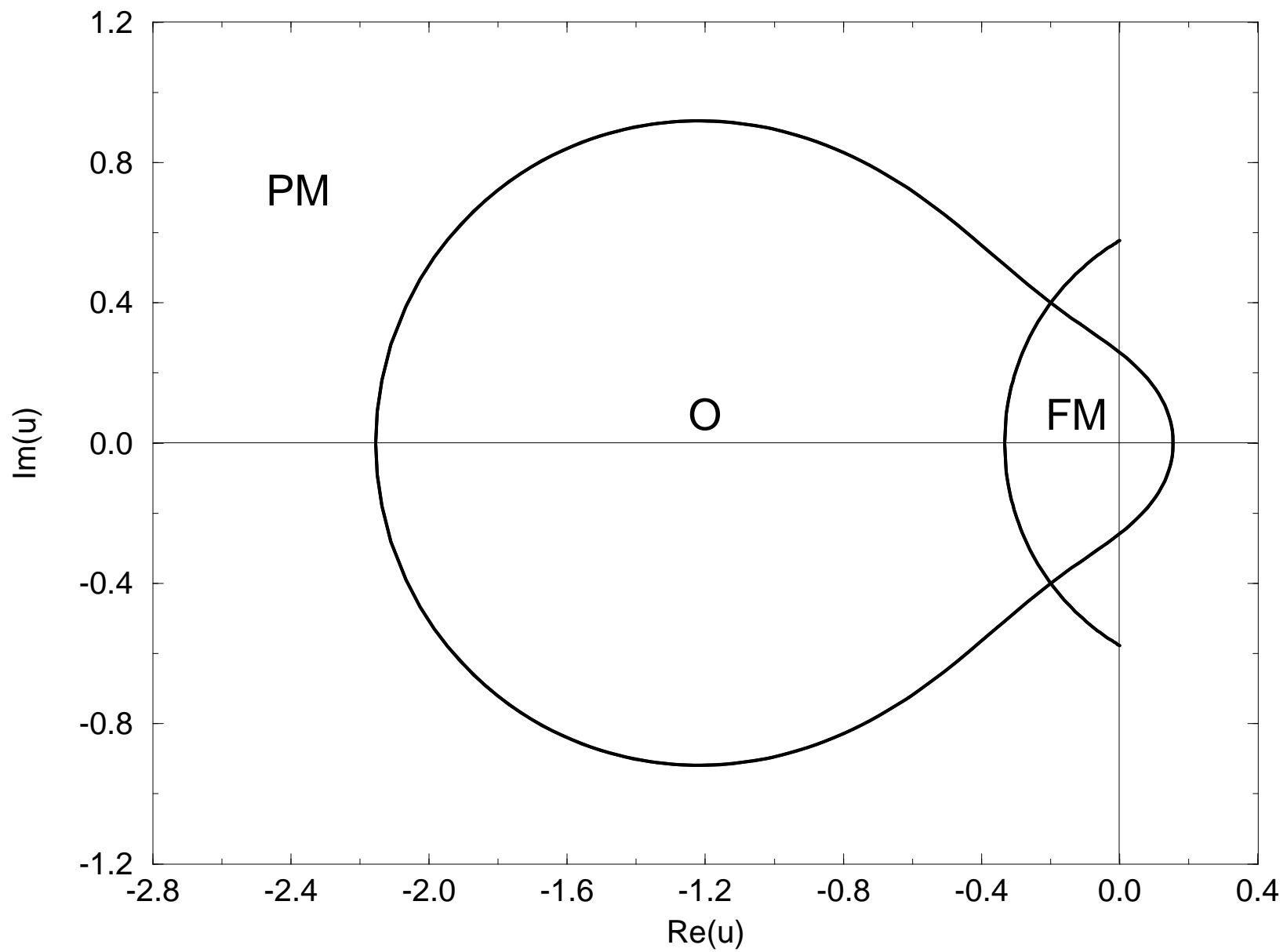
This figure "fig1-4.png" is available in "png" format from:

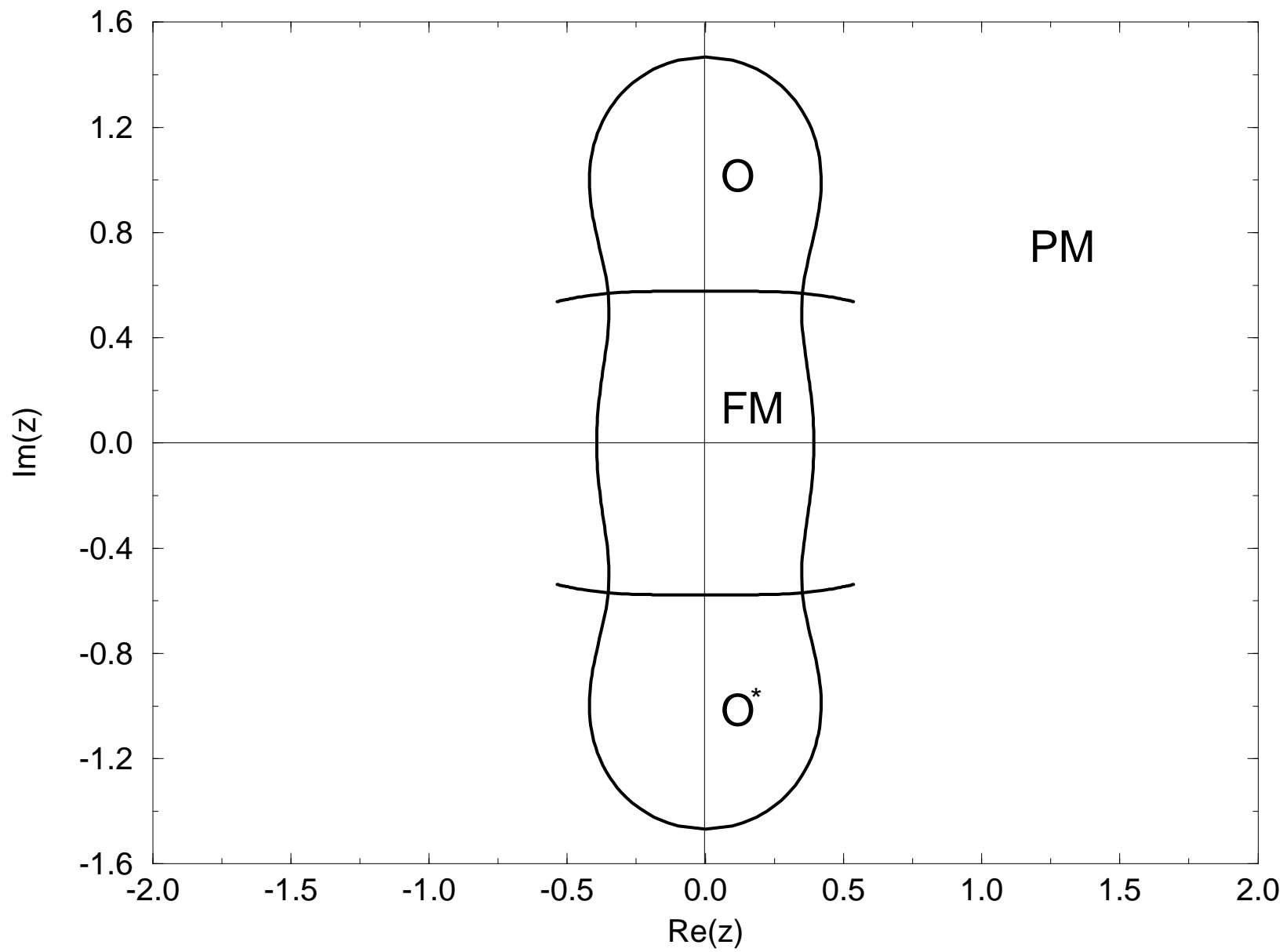
<http://arxiv.org/ps/hep-lat/9503005v1>

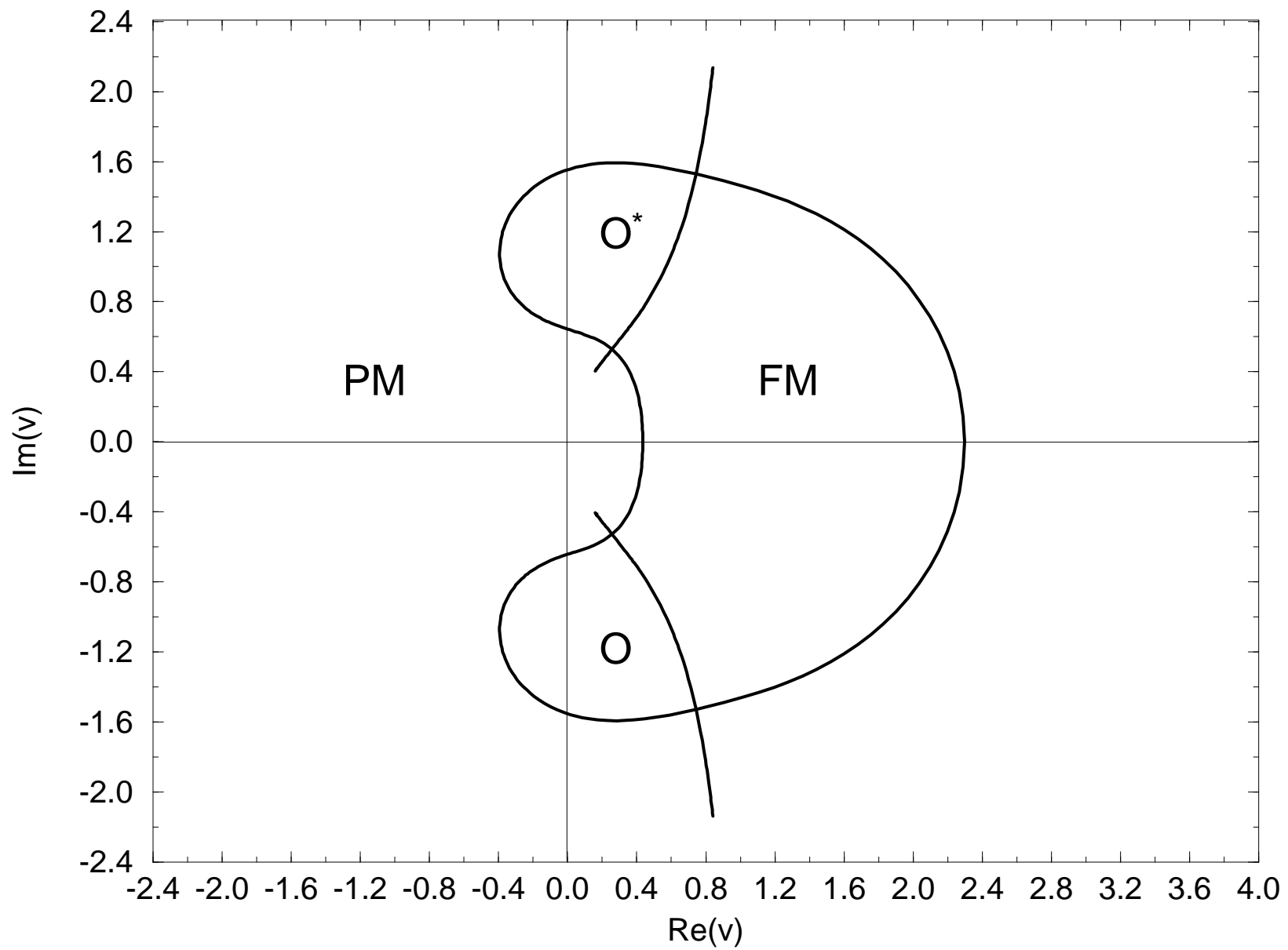


This figure "fig1-5.png" is available in "png" format from:

<http://arxiv.org/ps/hep-lat/9503005v1>

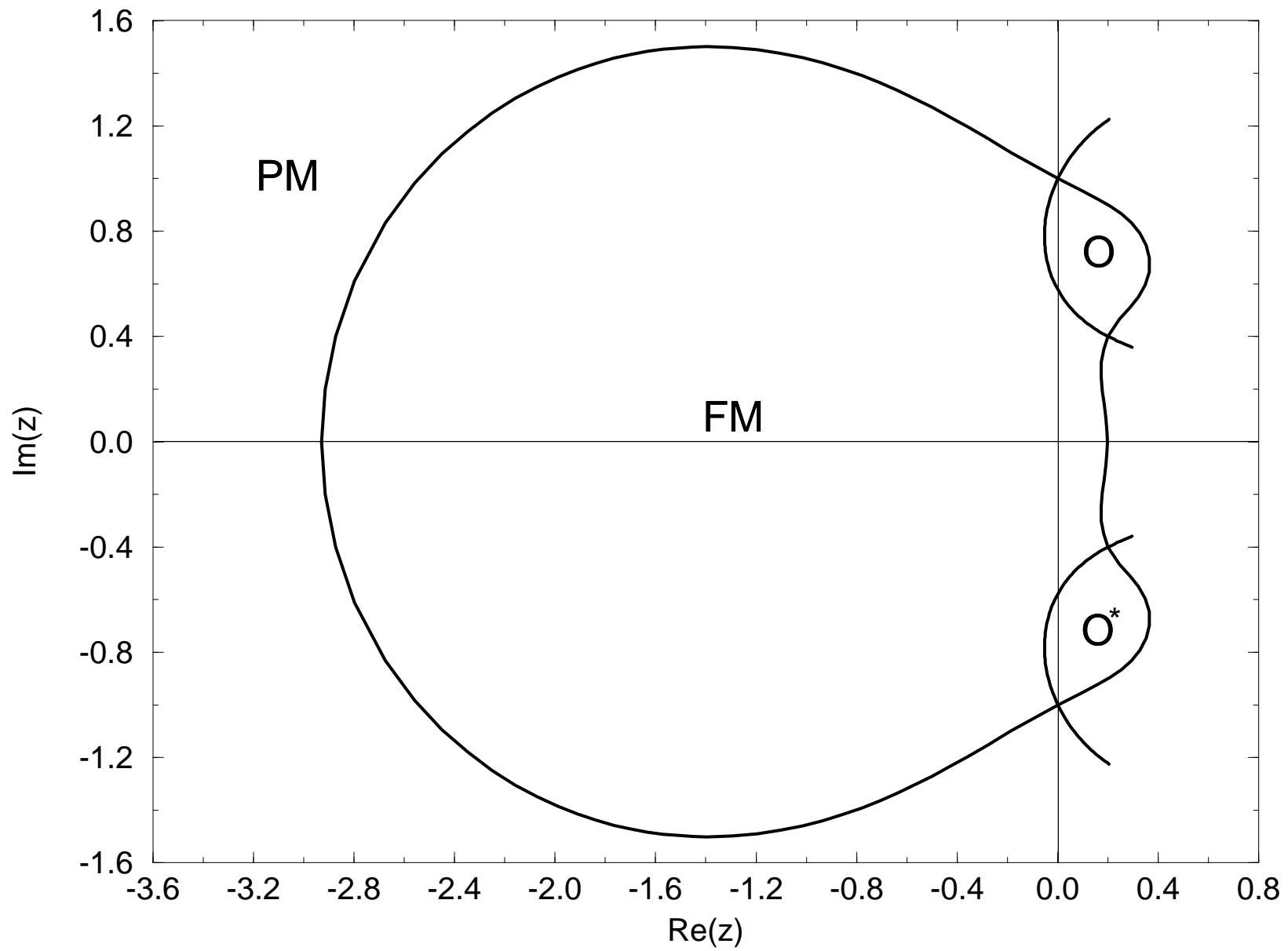


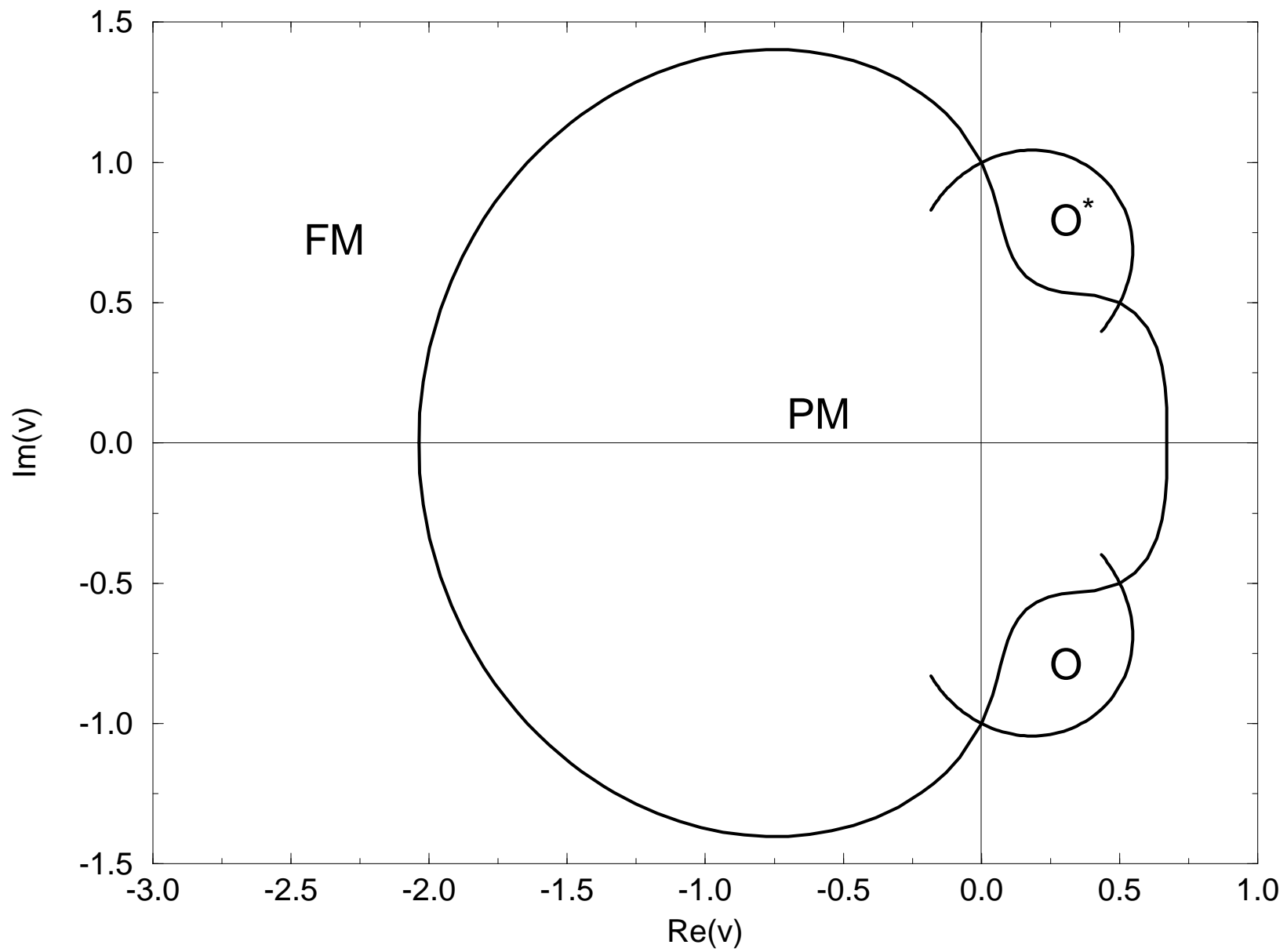




This figure "fig1-6.png" is available in "png" format from:

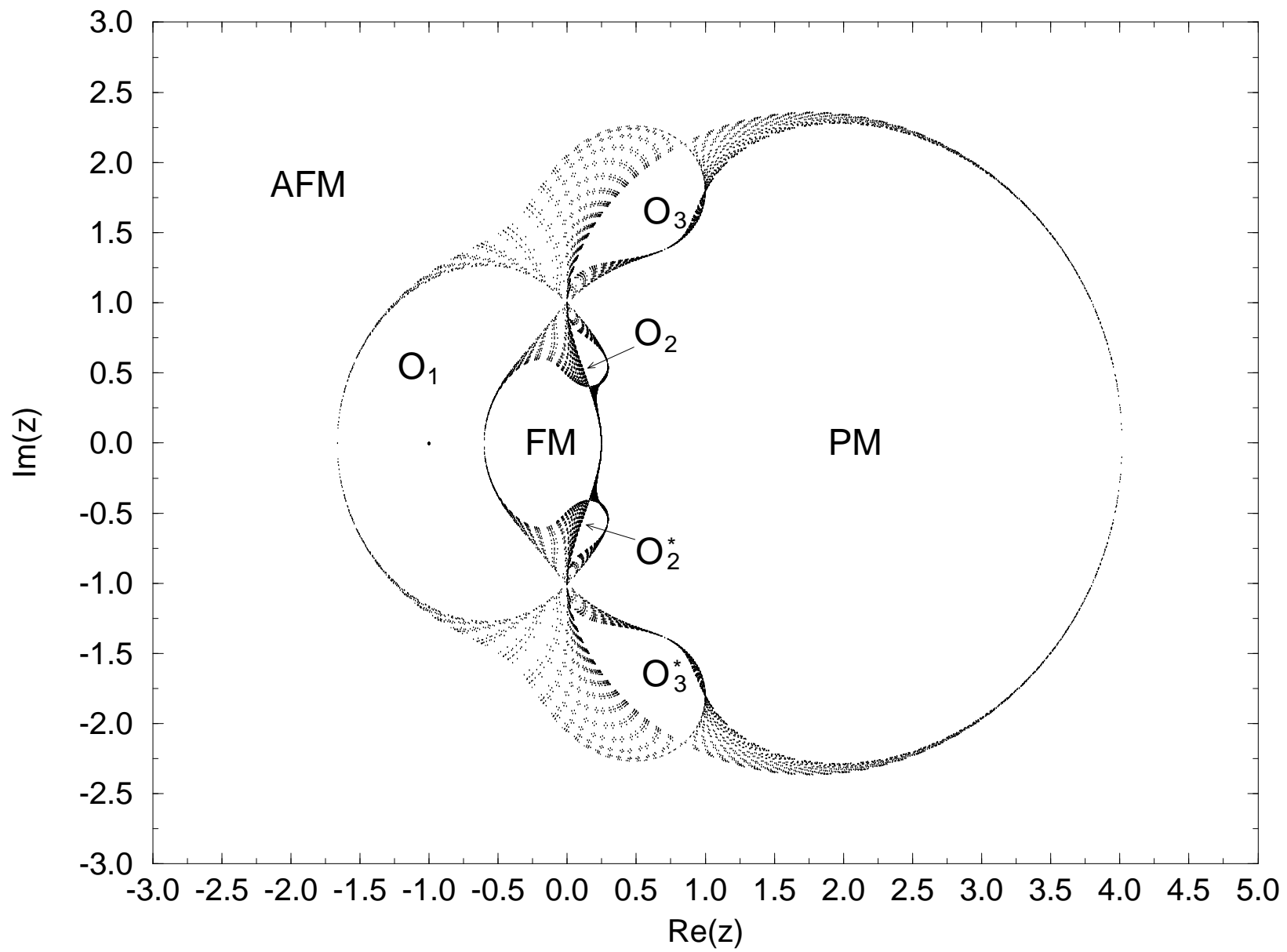
<http://arxiv.org/ps/hep-lat/9503005v1>

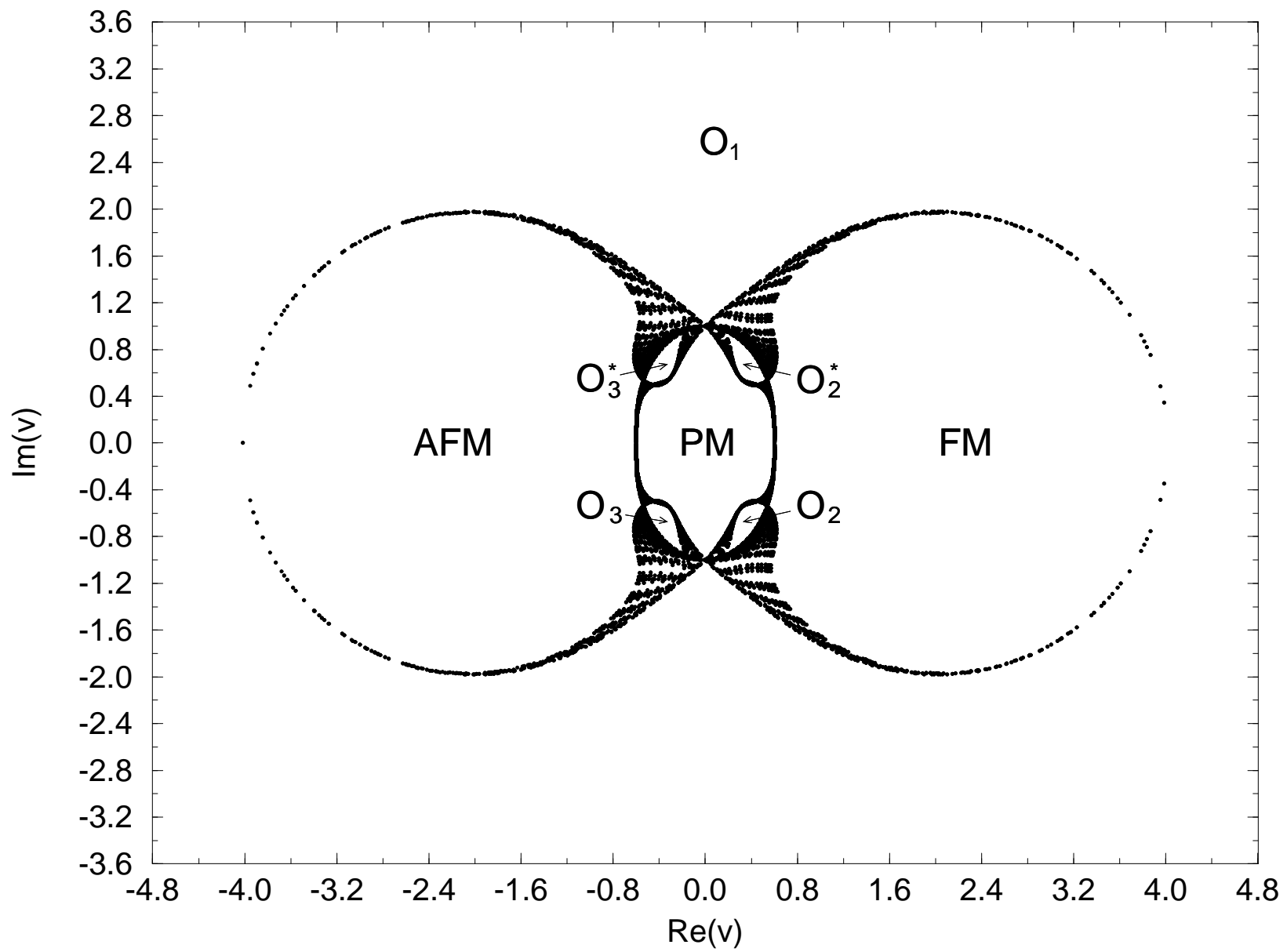




This figure "fig1-7.png" is available in "png" format from:

<http://arxiv.org/ps/hep-lat/9503005v1>





This figure "fig1-8.png" is available in "png" format from:

<http://arxiv.org/ps/hep-lat/9503005v1>

This figure "fig1-9.png" is available in "png" format from:

<http://arxiv.org/ps/hep-lat/9503005v1>

This figure "fig1-10.png" is available in "png" format from:

<http://arxiv.org/ps/hep-lat/9503005v1>

This figure "fig1-11.png" is available in "png" format from:

<http://arxiv.org/ps/hep-lat/9503005v1>